Interpretable Clinical Genomics with a Likelihood Ratio Paradigm

Peter N. Robinson,[1,2,*] Vida Ravanmehr,[1] Julius O.B. Jacobsen,[3] Daniel Danis,[1] Xingmin Aaron Zhang,[1,8] Leigh C. Carmody,[1] Michael A. Gargano,[1] Courtney L. Thaxton,[4] UNC Biocuration Core,[4] Guy Karlebach,[1] Justin Reese,[5] Manuel Holtgrewe,[6] Sebastian Köhler,[6] Julie A. McMurry,[7] Melissa A. Haendel,[7] and Damian Smedley[3]

Human Phenotype Ontology (HPO)-based analysis has become standard for genomic diagnostics of rare diseases. Current algorithms use a variety of semantic and statistical approaches to prioritize the typically long lists of genes with candidate pathogenic variants. These algorithms do not provide robust estimates of the strength of the predictions beyond the placement in a ranked list, nor do they provide measures of how much any individual phenotypic observation has contributed to the prioritization result. However, given that the overall success rate of genomic diagnostics is only around 25%–50% or less in many cohorts, a good ranking cannot be taken to imply that the gene or disease at rank one is necessarily a good candidate. Here, we present an approach to genomic diagnostics that exploits the likelihood ratio (LR) framework to provide an estimate of (1) the posttest probability of candidate diagnoses, (2) the LR for each observed HPO phenotype, and (3) the predicted pathogenicity of observed genotypes. LIkelihood Ratio Interpretation of Clinical AbnormaLities (LIRICAL) placed the correct diagnosis within the first three ranks in 92.9% of 384 case reports comprising 262 Mendelian diseases, and the correct diagnosis had a mean posttest probability of 67.3%. Simulations show that LIRICAL is robust to many typically encountered forms of genomic and phenomic noise. In summary, LIRICAL provides accurate, clinically interpretable results for phenotype-driven genomic diagnostics.

Introduction

Phenotype-driven prioritization of candidate genes and diseases is a well-established approach to genomic diagnostics in rare disease.[1–12] Most current approaches use the Human Phenotype Ontology (HPO) for annotating the set of phenotypic abnormalities observed in the individual being investigated by whole-exome or whole-genome sequencing. The HPO contains 14,813 terms arranged as a directed acyclic graph in which edges represent subclass relations; 13,182 of these terms represent phenotypic abnormalities. For instance, Abnormal renal cortex morphology (HP:0011035) is a subclass of Abnormal renal morphology (HP:0012210). The HPO project additionally provides computational disease models of 7,623 rare diseases that are constructed from HPO terms and metadata that define the diseases on the basis of the phenotypic abnormalities that characterize them, their modes of inheritance, and in many cases, the age of onset of diseases or phenotypic features and the overall frequencies of features in a disease.[13] For instance, Meckel syndrome type 7 is characterized by Patent ductus arteriosus (HP:0001643) with a frequency of two of seven affected individuals and Antenatal onset (HP:0030674).[14]

Diagnostic exome or genome sequencing typically reveals tens or hundreds of variants that are predicted to be deleterious by common computational frameworks, and therefore, the analysis of such data generally requires some additional criterion to prioritize genes.[15] Phenotypic approaches leverage the proband's observed phenotypic abnormalities to assess candidate diseases by searching diseases with similar phenotypic abnormalities that are associated with genes that harbor a predicted pathogenic variant.[16] However, current algorithms for phenotype-driven genomic diagnostics have a number of shortcomings that represent impediments to the successful implementation of genomic testing outside of specialist centers.

All current approaches that we are aware of present their results as an ordered list of candidate genes or diseases. The overall success rate of genomic diagnostics depends on the cohort and the next-generation sequencing (NGS) technique but is still hovering at about 40% for a wide range of conditions.[17–20] Therefore, one must expect that, in many cases, the top-ranked gene is actually not a good candidate. Also, existing approaches do not provide a framework for deciding how many candidates in the ranked list are worthy of detailed examination. Therefore, it would be desirable to provide a transparent measure of how good the top predictions are and why. Such an approach could reduce the number of candidates that busy diagnostic labs have to review. Finally, current approaches do not provide information about how much

[1]The Jackson Laboratory for Genomic Medicine, Farmington, CT 06032, USA; [2]Institute for Systems Genomics, University of Connecticut, Farmington, CT 06032, USA; [3]William Harvey Research Institute, Charterhouse Square, Barts and the London School of Medicine and Dentistry, Queen Mary University of London, London EC1M 6BQ, UK; [4]Department of Genetics, University of North Carolina, Chapel Hill, NC 27599, USA; [5]Environmental Genomics and Systems Biology, Lawrence Berkeley National Laboratory, Berkeley, CA, USA; [6]Charité Universitätsmedizin Berlin, Charitéplatz 1, 10117 Berlin, Germany; [7]Oregon State University, Corvallis, OR 97331, USA
[8]Present address: Sema4 Genomics (a Mount Sinai venture), Stamford, CT 06902, USA
*Correspondence: peter.robinson@jax.org
https://doi.org/10.1016/j.ajhg.2020.06.021.

individual phenotypic features contribute to the computational prediction. For clinical use, approaches that allow users to understand the reasons for the computational predictions are preferable to black-box algorithms and better support clinical decision making.[21]

In this work, we present an algorithm, LIkelihood Ratio Interpretation of Clinical AbnormaLities (LIRICAL), that calculates the likelihood ratio of each observed or excluded phenotypic abnormality. If genomic data is available, likelihood ratios are additionally calculated for genotypes. In contrast to previous approaches based on semantic similarity, LIRICAL provides an estimate of the posttest probability of candidate diagnoses. For each candidate diagnosis, LIRICAL calculates the extent to which each phenotypic abnormality (and if available genotype) is consistent with the diagnosis. To test the performance of LIRICAL, we generated simulated data from 384 published case reports and leveraged data from 116 solved cases from the 100,000 Genomes Project. LIRICAL was highly accurate and robust to several sources of noise.

Material and Methods

Data Sources

The hp/releases/2019-09-06 version of the HPO (hp.obo) was used for the analysis described here. The phenotype.hpoa file, containing HPO annotations (HPOA), was downloaded on October 16, 2019 from the HPO website.

Likelihood Ratio

The likelihood ratio (LR) is defined as the probability of a given test result (x) in an individual with a disease $\mathcal{D}$ divided by the probability of that same result in a person without the disease ($\neg\mathcal{D}$):

$$\mathrm{LR}(\mathrm{x}) = \frac{\Pr(\mathrm{x}|\mathcal{D})}{\Pr(\mathrm{x}|\neg\mathcal{D})} \qquad \text{(Equation 1)}$$

$\Pr(\mathrm{x}|\mathcal{D})$ is the sensitivity (true positive rate) of the test, i.e., the expected proportion of individuals with disease $\mathcal{D}$ who are correctly identified. The specificity or true negative rate is the proportion of individuals without disease $\mathcal{D}$ who are correctly identified as unaffected, i.e., $\Pr(\neg\mathrm{x}|\neg\mathcal{D})$. Therefore, the LR can be expressed as

$$\mathrm{LR}(\mathrm{x}) = \frac{\text{sensitivity}}{1-\text{specificity}} \qquad \text{(Equation 2)}$$

The definition of the LR can be extended to multiple tests.[22] Suppose $X = (x_1, x_2, \cdots, x_n)$ is an array of n test results. Under the assumption that the tests are independent, LR(X) is defined as

$$\frac{\Pr(X|\mathcal{D})}{\Pr(X|\neg\mathcal{D})} = \frac{\Pr(x_1, x_2, \cdots, x_n|\mathcal{D})}{\Pr(x_1, x_2, \cdots, x_n|\neg\mathcal{D})} = \prod_{i=1}^{n} \frac{\Pr(x_i|\mathcal{D})}{\Pr(x_i|\neg\mathcal{D})} \qquad \text{(Equation 3)}$$

The posttest probability refers to the probability that an individual has a disease given the information from test results X and the pretest probability of the disease. The posttest probability can be calculated as

$$\Pr(\mathcal{D}|X) = \frac{p\mathrm{LR}(X)}{(1-p) + p\mathrm{LR}(X)}, \qquad \text{(Equation 4)}$$

where p is the pretest probability of $\mathcal{D}$. Depending on the cohort, the pretest probability can be defined as the population prevalence of the disease or by some other estimate of the frequency of the disease in the cohort being tested.

LIRICAL calculates LRs for observed phenotypic abnormalities (HPO terms) and observed genotypes (as inferred from VCF files) by defining probability distributions for phenotypes and genotypes as described in the following sections.

LR for Phenotypes

The signs and symptoms and other phenotypic abnormalities of probands being investigated by this approach are represented using terms of the HPO, which provides a structured, comprehensive, and well-defined set of 14,813 classes (i.e., terms; September 2019 release) describing human phenotypic abnormalities.[13,23–25] We model the clinical encounter that results in a set of n phenotypic observations encoded as HPO terms $h_1, h_2, \ldots, h_n$. The LR of each phenotype term with respect to a specific disease $\mathcal{D}$ is defined as

$$\mathrm{LR}(h_i) = \frac{\Pr(h_i|\mathcal{D})}{\Pr(h_i|\neg\mathcal{D})}. \qquad \text{(Equation 5)}$$

We assume that the tests are independent and the LR of the n HPO terms can be obtained from the product of the individual ratios.

The Probability of Having Phenotypic Abnormality h_i Given a Disease $\mathcal{D}$

We first explain how we define the numerator of Equation 5 on the basis of the relationship of term h_i to the set of phenotype terms to which disease $\mathcal{D}$ is annotated (Figure S1). We distinguish seven cases, all of which are detailed in the following sections.

h_i Is Identical to One of the Terms to Which $\mathcal{D}$ Is Annotated

In this case, we define $\Pr(h_i|\mathcal{D}) = f_i^{\mathcal{D}}$, that is, the frequency of the phenotypic feature h_i among individuals with disease $\mathcal{D}$. For instance, if the disease model for $\mathcal{D}$ is based on a study in which seven of ten persons with $\mathcal{D}$ had h_i, then $f_i^{\mathcal{D}} = 0.7$. If no information is available about the frequency of h_i, then by default, we define $f_i^{\mathcal{D}} = 1$.

h_i Is an Ancestor of One or More of the Terms to Which $\mathcal{D}$ Is Annotated

Because of the annotation propagation rule of subclass hierarchies in ontologies,[26] $\mathcal{D}$ is implicitly annotated to all of the ancestors of the set of annotating terms. For instance, if the computational disease model of some disease $\mathcal{D}$ includes the HPO term polar cataract (HP:0010696), then the disease is implicitly annotated to the parent term cataract (HP:0000518) (to see this, consider that any person with a polar cataract can also be said to have a cataract). By extension, this is also true of more distant ancestors of the term. We therefore define the probability of a term h_i (e.g., cataract) that is an ancestor of any term h_j (e.g., polar cataract) that explicitly annotates disease $\mathcal{D}$ as

$$\Pr(h_i|\mathcal{D}) = \max_j f_j^{\mathcal{D}} \text{ such that } h_i \in \mathrm{anc}(h_j) \text{ and } h_j \in \mathrm{annot}(\mathcal{D}) \qquad \text{(Equation 6)}$$

where $anc(h_j)$ is a function that returns the set of all ancestors of term h_j and $annot(\mathcal{D})$ is a function that returns the set of all HPO terms that explicitly annotate disease $\mathcal{D}$. In other words, the probability of h_i in disease $\mathcal{D}$ is equal to the maximum frequency of any of the descendants of h_i that directly annotate disease $\mathcal{D}$.

h_i Is a Child Term of One or More of the Terms to Which $\mathcal{D}$ Is Annotated

In this case, h_i is a child (i.e., a specific subclass) of some term h_j that directly annotates $\mathcal{D}$. For instance, disease $\mathcal{D}$ might be annotated to syncope (HP:0001279), and the query term h_i is

orthostatic syncope (HP:0012670), which is a child term of syncope. In addition, syncope has two other child terms, carotid sinus syncope (HP:0012669) and vasovagal syncope (HP:0012668). According to our model, we will weight the frequency of syncope in disease $\mathcal{D}$ (say, 0.72) by $(1/|\text{child}(h_j)|)$, where $\text{child}(h_j)$ is the set of child terms of h_j (so in our example, we would use the frequency $0.72 \times 1/3 = 0.24$). In our implementation, only the direct children of a disease-associated term h_j are considered. The maximum frequency ($f_j^{\mathcal{D}}$) is taken across all disease-associated terms.

$$\Pr(h_i|\mathcal{D}) = \frac{1}{|child(h_j)|} \cdot \max_j f_j^{\mathcal{D}} \text{ such that } h_i \in \text{child}(h_j) \text{ and } h_j \in \text{annot}(\mathcal{D}) \quad \text{(Equation 7)}$$

where $child(h_j)$ refers to the set of direct descendants (child terms) of HPO term h_j. This algorithm is a heuristic whose intuition is that if a proband is annotated to a specific subterm of a term used to annotate a disease, this is not an exact match and should be penalized to some extent. If the proband is annotated to a term that is separated by more than one link from the disease term, then this heuristic does not consider it to be a match.

h_i and Some Term to Which $\mathcal{D}$ Is Annotated Have a Non-root Common Ancestor

In this case, h_i is not a child term of any disease term h_j and no disease term h_j is a descendant of h_i. LIRICAL then finds the closest common ancestor of h_i and all terms that annotate $\mathcal{D}$ (denoted h_{ca} in the following). Noting that h_{ca} might have a zero or very small frequency in disease $\mathcal{D}$, we define the LR using the following heuristic:

$$\text{LR}(h_i) = \frac{\Pr(h_{ca}|\mathcal{D})}{\Pr(h_{ca}|\neg\mathcal{D})} = \max\left(\frac{1}{100}, \frac{f_{ca}^{\mathcal{D}}}{\Pr(h_{ca}|\neg\mathcal{D})}\right)$$

Because the common ancestor is higher up in the HPO hierarchy, the LR tends to be lower and sometimes substantially lower for features with a high frequency across the HPO corpus [with a corresponding low value for $\Pr(h_{ca}|\neg\mathcal{D})$]. Therefore, in order to avoid a single term's having an excessive influence on the final result, the LR is taken to be at least $(1/100)$.

h_i Does Not Have Any Non-root Common Ancestor with Any Term to Which $\mathcal{D}$ Is Annotated

In this case, h_i does not affect the same organ system as any of the annotations of $\mathcal{D}$. A heuristic small value of $(1/100)$ is assigned.

The Proband Has a Phenotypic Abnormality h_i That Is Explicitly Excluded from Disease $\mathcal{D}$

In the HPO annotation resource, each disease is represented by a list of HPO terms that characterize it together with metadata, including provenance, and in some cases, frequency and onset information.[13] Some diseases additionally have explicitly excluded terms (there are a total of 921 such annotations in the September 2019 release of the HPOA data). These annotations are used for phenotypic abnormalities that are important for the differential diagnosis. For instance, Marfan syndrome and Loeys-Dietz syndrome share many phenotypic abnormalities.[27] The feature ectopia lentis (HP:0001083) is characteristic of Marfan syndrome but is not found in Loeys-Dietz syndrome.[28] The LR for such query terms is assigned an arbitrary value of $(1/1,000)$, i.e., the ratio for a candidate diagnosis is reduced by a factor of one thousand if an HPO term is present in the proband that is explicitly excluded from the disease.

The Proband Was Shown Not to Have a Phenotypic Abnormality h_i That Is Explicitly Excluded from Disease $\mathcal{D}$

On the other hand, if the query includes a negated term that is explicitly excluded in the disease, then the opposite value is assigned, i.e., the ratio for a candidate diagnosis is increased by a factor of one thousand if an HPO term is present in the proband that is explicitly excluded from the disease.

The Probability of Having Phenotypic Abnormality h_i if Disease $\mathcal{D}$ Is Not Present

The denominator of Equation 5 specifies the probability of the test result given that the proband does not have some disease $\mathcal{D}$. This would be difficult to calculate for the general population for the same reasons as those described above. However, we can estimate this probability if we assume that all persons being tested have some (unknown) Mendelian disorder by simply summing over the overall frequency of a feature in the entire HPO corpus (with N diseases).

$$\Pr(h_i|\neg D_j) = \frac{1}{(N-1)} \sum_{k \neq j} \Pr(h_i|D_k) = \frac{1}{(N-1)} \sum_{k \neq j} f_i^{D_k} \quad \text{(Equation 8)}$$

Equation 8 would need to be calculated separately for each of the N diseases, but noting that we are summing over a relatively large number of diseases (7,623 in September, 2019) in the complete HPO database of rare diseases, we use the following approximation that allows us to precalculate $\Pr(h_i|\neg D_j)$ for an arbitrary disease D_j.

$$\Pr(h_i|\neg D_j) \approx \frac{1}{N} \sum_{k=1}^{N} f_i^{D_k} \quad \text{(Equation 9)}$$

Likelihood Ratio for Genotypes

Our model of predicting the relevance of any given genotype makes use of the following concepts. We define the genotype of each specific gene with $0, \ldots, n$ variants located in the gene on the basis of the set of heterozygous or homozygous calls for each observed variant as derived from a Variant Call Format (VCF) file.

There is a true but unobservable pathogenicity of each variant, defined as a deleterious effect on the biochemical function of a gene and the gene product it encodes, that leads to disease. We can estimate the pathogenicity of a variant on the basis of a computational pathogenicity score that ranges from 0 (predicted benign) to 1 (maximum pathogenicity prediction). Our model posits two distributions that allow us to calculate the likelihoods of an observed genotype given that the sequenced individual has the disease $(\mathcal{D})$ as compared to the situation in which the individual does not have the disease in question and the variants originate from population background ($\mathcal{B}$; that is, the variants are called pathogenic by bioinformatic analysis but are not related to the disease in question).

We use the pathogenicity score of the Exomiser, which calculates a score for any variant in the coding exome or at the highly conserved dinucleotide sequences at either end of introns. Exomiser pathogenicity scores are assigned via a variety of pathogenicity predictors—usually a combination of PolyPhen, SIFT, and MutationTaster for missense mutations, heuristics for other classes of variant, and membership of the variant in a high-confidence pathogenic or likely pathogenic ClinVar dataset. The highest (most deleterious) normalized score of these is used as the

Exomiser pathogenicity score.[4,29] We use the estimated population frequencies of variants from gnomAD,[30] which is incorporated into the Exomiser database, to calculate the background distribution (version 12.1.0 was used for the analysis reported here).

Our model depends on the assumed mode of inheritance of the disease; we will begin our explanation with autosomal-dominant (AD) diseases. We are interested in the ratio of an observed genotype ($\mathcal{G}$) given that it is disease causing (i.e., the sequenced individual has disease $\mathcal{D}$) or not disease causing (i.e., the sequenced individual does not have disease $\mathcal{D}$). Assume we observe n variants $(v_1, v_2, \ldots, v_n)$ in gene g and have calculated their pathogenicity score as $s(v_i)$ for $i \in \{1, \ldots, n\}$. For simplicity, we will assume that the variants have been arranged such that $s(v_1) \geq s(v_2) \geq \ldots \geq s(v_n)$.

We first note that 98.9% of the pathogenicity scores of variants classified as pathogenic in ClinVar[31] are assigned a pathogenicity score of 0.8 or more by Exomiser (Figure S2). For the purposes of assessing and scoring candidate variants, we therefore divide the score distribution into two bins, $\mathcal{N}$ and $\mathcal{P}$; bin $\mathcal{N}$ represents the predicted non-pathogenic bin and has a range of pathogenicity scores of $[0, 0.8)$, and bin $\mathcal{P}$ represents the predicted pathogenic bin with pathogenicity scores of $[0.8, 1]$. That is, $\mathcal{P}$ represents the bioinformatic prediction of whether a variant is "pathogenic." In general, it is not possible to know with certainty whether any variant (be it in bin $\mathcal{N}$ or $\mathcal{P}$) is causally related to a disease or phenotype.

In other words, LIRICAL models variants into two bins, $\mathcal{N}$ and $\mathcal{P}$. Variants in $\mathcal{N}$ are discarded. Variants in $\mathcal{P}$ are modeled as coming from two distributions, $\mathcal{D}$ (disease-related) and $\mathcal{B}$ (background). The purpose of this scheme is to downweight variants in genes that often show predicted pathogenic variants and tend to be frequently found as false positives in exome sequencing results, such as many mucin and HLA genes.[32]

LIRICAL's Genotype Concept

The word "genotype" is used with different meanings in different contexts. Unless we specifically refer to the genotype of a variant (e.g., homozygous reference, heterozygous, homozygous alternate), in the following text we define "genotype" as follows. For each gene that is associated with a candidate disease, LIRICAL takes into account the predicted pathogenicity and genotype of each variant. For instance, if three variants are observed in a gene g and the first two are heterozygous (0/1) and the third is homozygous ALT (1/1), then LIRICAL defines the genotype of g to be

$$\mathrm{gt}(g) = [(0/1, s(v_1)), (0/1, s(v_2)), (1/1, s(v_3))] \quad \text{(Equation 10)}$$

LIRICAL's Genotype Model

We model the expected counts of observed alleles in bin $\mathcal{P}$ as Poisson distributions, using separate distributions for the case that a variation in a given gene is disease causing or not. In this context, a Poisson distribution gives the probability of observing k variants in a gene, based on a rate parameter λ that represents the expected number of variants.

$$\Pr(k) = \mathrm{Pois}(k; \lambda) = e^{-\lambda}\frac{\lambda^k}{k!} \quad \text{(Equation 11)}$$

For an AD disease associated with pathogenic variants in gene g, we expect one heterozygous disease-causing variant, and so $\lambda^{\mathcal{D}_g} = 1$; for autosomal-recessive diseases, $\lambda^{\mathcal{D}_g} = 2$. We can estimate the probability of observing a variant in bin $\mathcal{P}$ in a gene g that is not related to the disease on the basis of the frequency of such variants in the general population; we denote this probability as $\lambda^{\mathcal{B}_g}$. Different genes have different distributions of predicted pathogenic variants in the general population. If a gene has a low frequency of predicted-pathogenic variants in the general population, then the observation of a predicted-pathogenic variant in a diagnostic context might be more likely to be a true-positive disease-causing variant.[33] We calculate $\lambda^{\mathcal{B}_g}$ for each gene g on the basis of available population frequency data from the gnomAD[30] resource by summing up the frequencies of individual variants under the independence assumption.

In detail, the frequency (if available) of each variant allele is taken from each of the following populations: African/African American (GNOMAD_E_AFR), Admixed American (GNOMAD_E_AMR), Ashkenazi Jewish (GNOMAD_E_ASJ), East Asian (GNOMAD_E_EAS), Finnish (GNOMAD_E_FIN), Non-Finnish European (GNOMAD_E_NFE), and South Asian (GNOMAD_E_SAS). For the analysis reported here, the average frequency in all populations is calculated. We note that this approach might overestimate the overall frequency of variants per exome or genome, but nonetheless we can use it as a heuristic to downweight genes commonly found to have predicted-pathogenic variants in the population (e.g., Table S1), as we will show below.

We denote the function that returns the predicted pathogenicity of a variant as path and the function that returns the average population frequency of a variant allele as freq. We represent the fact that variant i is assigned to gene g as $v_i \in g$.

$$\lambda^{\mathcal{B}_g} = \sum_{v_i} \mathrm{freq}(v_i) + \epsilon \text{ for } v_i \in g \text{ and } \mathrm{path}(v_i) \in \mathcal{P} \quad \text{(Equation 12)}$$

The parameter $\lambda^{\mathcal{B}_g}$ is thus the expected count of variant alleles in gene g whose pathogenicity score is in bin $\mathcal{P}$. A small number ($\epsilon = 10^{-5}$) is added to the sum to avoid division by zero in subsequent steps because some genes did not display any variants in bin $\mathcal{P}$ in the population data.

LIRICAL provides files with $\lambda^{\mathcal{B}_g}$ values for hg19 and hg38 (background-hg19.tsv and background-hg38.tsv). The file appropriate for the VCF file being analyzed is used automatically, but users can provide custom background files if desired. The code used to generate the background files is provided as a part of the LIRICAL distribution.

Genotype LR for Genes Associated with AD Diseases

For a gene associated with an AD disease, the calculation proceeds as follows. Assume we are evaluating disease $\mathcal{D}$, which is associated with mutations in gene g, and that there is one predicted-pathogenic variant v' in bin $\mathcal{P}$ and there are k other predicted-non-pathogenic variants in bin $\mathcal{N}$. The model assumes that any variants in bin $\mathcal{N}$ are unrelated to the disease and have the same probability whether or not gene g is causally related to the disease. That is, for a variant $v_i' \in \mathcal{N}$, $\Pr(v_i'|\mathcal{D}) = \Pr(v_i'|\neg\mathcal{D})$. The genotype observed for gene g is symbolized as $gt(g)$.

$$\mathrm{LR}(gt(g)) = \frac{\Pr(gt(g)|\mathcal{D})}{\Pr(gt(g)|\neg\mathcal{D})}$$

$$= \frac{\Pr(v'|\mathcal{D})}{\Pr(v'|\neg\mathcal{D})} \times \prod_{\substack{i \\ v_i \neq v'}} \frac{\Pr(v_i|\neg\mathcal{D})}{\Pr(v_i|\neg\mathcal{D})}$$

$$= \frac{\Pr(v'|\mathcal{D})}{\Pr(v'|\neg\mathcal{D})}$$

We model the process by which a variant or variants lead to disease by a compound distribution. A Poisson distribution models the number of variants observed whose pathogenicity score is in

bin $\mathcal{P}$, and a Bernoulli distribution with parameter $p = s(v')$ determines the probability that the allele is disease causing. Thus, let $\{\mathbf{X}_n\}$ be a sequence of mutually independent random variables each of which can take on the value of 0 (for not disease-causing) or 1 (for disease-causing). The sum of N such variables is $S_N = X_1 + X_2 + \ldots + X_n$, and thus, S_N represents the count of truly pathogenic alleles (we expect $S_N = 1$ for AD diseases and $S_N = 2$ for autosomal-recessive diseases).

This leads to the compound distribution

$$\Pr\{S_n = k\} = \text{Binom}(k; n, p)\text{Pois}(k; \lambda) \qquad \text{(Equation 13)}$$

It can be shown that this is equivalent to a Poisson distribution with parameter λp.[34] Therefore, to calculate the LR, we substitute the parameters $\lambda^{\mathcal{D}_g}$ and $\lambda^{\mathcal{B}_g}$ as well as $p_i = s(v_i)$.

$$\text{LR}(g) = \frac{\Pr(v'|\mathcal{D})}{\Pr(v'|\mathcal{B})} = \frac{\text{Pois}\left(1; p_i\lambda^{\mathcal{D}_g}\right)}{\text{Pois}\left(1; p_i\lambda^{\mathcal{B}_g}\right)} \qquad \text{(Equation 14)}$$

To calculate Equation 14, LIRICAL extracts the value of $\lambda^{\mathcal{B}_g}$ from the corresponding background frequency file (see above). The value of p_i is calculated on the basis of the corresponding Exomiser pathogenicity scores. Finally, $\lambda^{\mathcal{D}_g} = 1$ for AD diseases and $\lambda^{\mathcal{D}_g} = 2$ for autosomal-recessive diseases. Equation 14 will have the effect of favoring genes with a single heterozygous variant in bin $\mathcal{P}$ with a maximal pathogenicity score $(p_i = s(v') = 1)$ and that have a minimal frequency of bin $\mathcal{P}$ variant alleles in the population. If this is the case, then $\lambda^{\mathcal{B}_g} = \epsilon$ and we can calculate the LR by using Equation 11:

$$\text{LR}(g) = \frac{\text{Pois}(1; 1)}{\text{Pois}(1; \epsilon)} \approx 36788 \qquad \text{(Equation 15)}$$

LIRICAL does not calculate the LR for a gene unless at least one predicted-pathogenic variant is present (i.e., k is always at least 1). If more than the expected number of variants are found (say three predicted-pathogenic variants for an AD disease, where $\lambda^{\mathcal{D}_g} = 1$), the numerator of Equation 14 would be smaller, that is, $\text{Pois}(3; p_i\lambda^{\mathcal{D}_g}) < \text{Pois}(1; p_i\lambda^{\mathcal{D}_g})$.

Genotype LR for Genes Associated with Autosomal-Recessive Diseases

The procedure for autosomal-recessive diseases is analogous, except that $\lambda^{\mathcal{D}_g} = 2$. In the case that gene g is causative for the disease in the individual being sequenced, then we expect to find two alleles (which will be identical in case of a pathogenic homozygous variant and distinct in the compound heterozygous case). The two alleles in bin $\mathcal{P}$ with the highest pathogenicity score are chosen for analysis. Let s_{avg} denote the mean of the pathogenicity scores of the two variant alleles observed in gene g that have the two highest pathogenicity scores, i.e., $s_{avg} = 0.5 \cdot (s(v_1) + s(v_2))$. Then,

$$\text{LR}(gt(g)) = \frac{\Pr(v'|\mathcal{D})}{\Pr(v'|\neg\mathcal{D})} = \frac{\text{Pois}\left(2; s_{avg} \cdot \lambda^{\mathcal{D}_g}\right)}{\text{Pois}\left(2; s_{avg} \cdot \lambda^{\mathcal{B}_g}\right)} \qquad \text{(Equation 16)}$$

This will have the effect of favoring genes with a minimal frequency of bin $\mathcal{P}$ variants in the population and with two pathogenic alleles (homozygous or compound heterozygous) in bin $\mathcal{P}$, which have a maximal pathogenicity score $(s(v') = 1)$. In this case, $\lambda^{\mathcal{B}_g} = \epsilon$ and $\text{LR}(g) \approx 3,678,831,200$, but this value is not seen in practice.

If only one predicted-pathogenic variant is found in an autosomal-recessive disease, the numerator of Equation 16 is smaller than if two variants are present, i.e., $\text{Pois}(1; s_{avg} \cdot \lambda^{\mathcal{D}_g}) < \text{Pois}(2; s_{avg} \cdot \lambda^{\mathcal{D}_g})$. This has the effect of downweighting disease genes associated with recessive diseases for which only one heterozygous pathogenic allele is found but avoids filtering them out entirely.

In males, hemizygous variants on the X chromosome are called as homozygous by current variant-calling software. Therefore, we set $\lambda^{\mathcal{D}_g} = 2$ for both recessive and dominant X chromosomal diseases.

Genotype Likelihood Ratio: Special Cases

No Variants at All Found in Gene g

If the molecular basis of a disease is known to be mutations in a gene g, but no bin $\mathcal{P}$ variants or no variants at all are found in that gene, then an LR of 1/20 is assigned for AD diseases, reflecting an estimation that the probability of missing a pathogenic variant if one is present is about 5%. For autosomal-recessive diseases, we estimate the probability at $0.05 \times 0.05 = 0.0025$.

The motivation for this approach is that some downweighting should be performed if no candidate variant is found in a gene, but given the presumed high prevalence of false-negative results in exome/genome sequencing, it would not be desirable to radically downweight otherwise strong candidates.

Clinvar Pathogenic Variant(s) Found in Gene g

ClinVar[31] makes use of the American College of Medical Genetics and Genomics and the Association for Molecular Pathology standards for the interpretation of a variant as pathogenic (i.e., causative of a disease).[35] Denote the count of ClinVar pathogenic alleles as c. If $c = 2$ for autosomal-recessive diseases, then a heuristic LR of $1,000^2$ is assigned. If $c = 1$ for an AD disease, then a heuristic LR of 1,000 is assigned. If the c does not match the count of pathogenic alleles that would be expected for the mode of inheritance, then a heuristic LR of 1,000 is assigned.

This heuristic means that if a ClinVar pathogenic variant is found even in a gene, such as *TTN*, that is characterized by a high frequency of predicted-pathogenic variants in the population, then this is taken as being supportive of a diagnosis associated with variants in the gene.

Heuristic for Genes with Many Variants

Some genes commonly harbor variants in the general population that are predicted as pathogenic by bioinformatic software (cf. Figure S3 and Table S1). LIRICAL uses the background score to assess this. The background score ranged from 0 to 20.7 (for *MUC4*). Numerous disease-associated genes displayed scores over 1.0, including, for example, *TTN*, which had a score of 9.5. According to our model, it is not surprising to observe a predicted-pathogenic variant in a gene such as *TTN* whether or not the gene is associated with the disease being investigated in any particular case. LIRICAL downweights the LR for genotypes in these genes if predicted-pathogenic variants are found in a VCF file because such variants are commonly encountered as false positive findings.[15] It does so by limiting the value of $\lambda_g^{\mathcal{B}}$ to be at most the observed count of predicted-pathogenic variants, c_{path}, in cases where $\lambda_g^{\mathcal{B}} \geq 1$ (if the observed called-pathogenic variant count is much higher, the probability calculated by the Poisson distribution will be very low).

$$\lambda_g^{\mathcal{B}} := \min\left(c_{path}, \lambda_g^{\mathcal{B}}\right).$$

For instance, if one predicted-pathogenic variant is identified in *TTN*, this scheme would lead to an LR of one—the observation of the predicted-pathogenic variant in this gene neither adds to nor detracts from the probability of the differential diagnosis (we treat known disease-associated variants in ClinVar differently, see above).

–global Setting for Genotype Likelihood Ratio

Our approach has two options for dealing with genes in which no predicted pathogenic variants are observed. With the default option, LIRICAL will remove the genes and the diseases they are associated with from further analysis. This might be most appropriate if the goal of analysis is to demonstrate the genetic etiology of a disease.

If the –global option is chosen, LIRICAL ranks all diseases (including those with and without known associated disease genes) according to the posttest probability. In this case, if a disease has no associated disease gene, the LR is calculated from the phenotype evidence alone. Our procedure is designed to work whether or not genetic evidence is available to support a candidate diagnosis. If, for instance, the individual being sequenced is affected by a Mendelian disease for which the causative genes have not yet been identified, then, if there is a good phenotypic match, ideally the analysis procedure would include the disease in the overall results. Therefore, we omit the genotype score from the overall LR for Mendelian diseases in the HPO database that have a currently unclarified molecular basis.

Combined Genotype-Phenotype Likelihood Ratio Score

Our procedure takes as input a VCF file and a list of HPO terms representing the set of phenotypic abnormalities observed in the individual being sequenced. For each of the ~4,300 Mendelian diseases in the HPO database for which the causative disease gene has been identified, all predicted-pathogenic variants are extracted and the corresponding genotype LR is calculated. The LRs are calculated for each phenotypic feature as described above. The final LR for some disease $\mathcal{D}$ is then

$$\mathrm{LR}(\mathcal{D}) = \mathrm{LR}(gt(g)) \times \prod_i \frac{\Pr(h_i|\mathcal{D})}{\Pr(h_i|\neg\mathcal{D})} \qquad \text{(Equation 17)}$$

Ranking Candidates

Our approach calculates the LR of Equation 17 for each disease represented in the HPO disease database ($n = 7,623$ in the 9/2019 release). By default, LIRICAL uses disease definitions derived from the Online Mendelian Inheritance in Man (OMIM) knowledge resource.[36] This definition of disease treats each disease-gene pair as a unique disease (e.g., each of the ten forms of Hermansky-Pudlak syndrome are treated as a unique disease). LIRICAL can also be run using phenotype annotations derived from Orphanet[37] by using the –orpha flag. Orphanet defines diseases based on clinical considerations, whatever the number and nature of the causes (i.e., number of causative genes, different modes of inheritance, etc.),[38] and so in this example, there is only one disease code for Hermansky-Pudlak syndrome.

Finally, LIRICAL ranks diseases according to their posttest probability as calculated by Equation 4.

Visualization

The results of analysis are displayed here by showing bars whose magnitude is proportional to the decadic logarithm of the LRs of each tested feature. Features that support the differential diagnosis are shown in green and directed to the right of a vertical line in the center of the plot, and features that speak against the differential diagnosis are shown in red and directed to the left.

Evaluation

We curated HPO terms from 384 published case reports (Tables 1 and S2). We chose case reports in which the causative mutation had been identified so that we could perform simulations with and without a simulated exome. For each case report, we strove to capture all of the phenotypic features that were observed or explicitly excluded with corresponding HPO terms. The variants reported in the case reports were recorded via hg19 coordinates and checked via VariantValidator.[39]

We downloaded the file project.NIST.hc.snps.indels.vcf from the Genome in a Bottle project website.[40] This file contains variant calls derived from Illumina short-read exome sequencing of the samples NIST7035 and NIST7086. We used bcftools[41] to create a VCF file with NIST7035 as the single sample. For each phenopacket, the causative mutation or mutations were spiked into the VCF file.

We compared the results of simulation with the original data and also performed various types of obfuscation to assess the influence of noise on the performance of LIRICAL and Exomiser, adding varying degrees of phenotypic or genotypic noise (Table S3).

A comparison of LIRICAL and Exomiser was also performed for 116 solved cases from the 100,000 Genomes Project for which detailed clinical phenotype data in the form of HPO terms had been collected. All cases were singletons with single-sample VCF files available. The diagnoses came from 89 different genes across a wide spectrum of rare disease areas (cardiovascular, ciliopathies, dermatological, dysmorphic and congenital abnormalities, endocrine, hearing and ear, metabolic, neurology and neurodevelopmental, ophthalmological, renal and urinary tract, rheumatological, skeletal, and tumor syndromes).

Implementation

LIRICAL is implemented as a Java application. It is written in Java 1.8 and compiles under Java 11. An executable and source code can be downloaded from the GitHub page, and detailed documentation is available at the read the docs page (see Web Resources). LIRICAL is freely available for academic use.

Results

In this work, we present an approach to clinically interpretable prioritization of candidate diseases based on the LR framework. The LR is defined as the probability of a given test result in an individual with the target disorder divided by the probability of that same result in an individual without the target disorder. The LR framework allows multiple test results to be combined by multiplying the individual ratios and also relates the pretest probability to the posttest probability in a way that can be used to guide clinical decision making.[22,42,43]

The LIRICAL Algorithm

We define an LR-based model of the clinical examination of an individual being investigated for a suspected but unknown Mendelian disorder as follows. Each recorded phenotypic observation is defined as a clinical test. The probability that a person with disease $\mathcal{D}$ has a phenotypic abnormality encoded by HPO term h_i, denoted as $f_i^{\mathcal{D}}$, is taken to be the

Table 1. Phenopackets Used for Evaluating the Performance of LIRICAL

Total case reports	384
Diseases	
Median # cases per disease	1
Maximum # cases per disease	19
Autosomal-recessive diseases	203
Autosomal-dominant diseases	128
X chromosomal diseases	10
Multiple modes of inheritance	43
Total	262
Disease genes	
Total	259
HPO terms	
Total over all cases	1687
Mean # HPO terms per case	11.1 (median 9)
Mean # negated HPO terms per case	2.71 (median 0)

384 phenopackets each describing a single published case report were derived from the literature by manual biocuration. See Table S2 for details. Multiple modes of inheritance means that more than one mode has been described for the disease in question, e.g., inherited cataract associated with variants in *PITX3* can be inherited in an autosomal-dominant or autosomal-recessive fashion. The phenopacket schema represents an open standard for sharing machine-readable phenotypic descriptions in the context of rare disease, common disease, or cancer (see Web Resources).

frequency with which the abnormality is observed in affected individuals as recorded in the computational disease models of the HPO project based on literature biocuration (a default value of 100% is used if specific frequency information is not available). For many diseases and features, an overall frequency of the feature is known; for instance, 19/437 persons ($\sim 4\%$) with neurofibromatosis type 1 have seizures.[44] On the other hand, 338/442 individuals ($\sim 87\%$) with this disease have multiple café-au-lait spots.[45] In our algorithm $f_i^{\mathcal{D}}$ represents the numerator of the LR.

The denominator of the LR is the probability of the phenotypic feature if the proband does not have the disease ($\mathcal{D}$) in question. It would be difficult to calculate this for each of the 13,182 phenotypic abnormalities of the HPO in the general population, but we note that a tractable and realistic model for our purposes is that any proband being investigated by genomic diagnostics has some genetic disease. We can therefore calculate the denominator of the LR by means of the overall prevalence of HPO feature h_i in genetic diseases other than $\mathcal{D}$. For instance, if $\mathcal{D}$ and 13 of the 7,622 other diseases in the HPO database are characterized by feature h_i and we assume an equal pretest probability for all diseases, then the probability of the proband's having feature h_i if the proband is not affected by disease $\mathcal{D}$ is the sum of the frequencies of h_i in the 13 diseases divided by 7,622 (an efficient approximation of this probability is used; see Methods).

Our algorithm takes as input a VCF file with genetic variants identified in an exome, genome, or gene panel experiment as well as a list of HPO terms that describe the phenotypic abnormalities observed in the proband. The algorithm returns a ranked list of candidate diagnoses each of which is assigned a posttest probability. Each of the HPO terms is conceived of as a diagnostic test, and an LR is calculated for each term, representing the probability that a proband has the term in question if the proband has the candidate disease divided by the probability of the proband's having the term if the proband does not have the candidate disease.

The current version of the HPO database comprises 7,623 diseases of which 5,192 are associated with at least one gene (total disease-associated genes: 4,025) and 2,431 diseases are not associated with a gene. In contrast to previous approaches to phenotype-driven genomic diagnostics,[1,2,29] our approach includes diseases with no known disease-associated gene in the differential. However, if a disease-associated gene is known, then the genotype of the proband is also used as a diagnostic test in the LR framework. The LR is calculated for the observed genotype of the gene on the basis of our expectation of observing one or two causative alleles according to the mode of inheritance of the disease and also the probability of observing called pathogenic variants in the gene in the general population. The individual LRs are multiplied to obtain a composite LR, which, together with the pretest probability of each disease, is used to calculate the posttest probability in order to rank the diseases.

LIRICAL Supports Clinical Interpretation with Estimates of Posttest Probability and Per-phenotype LRs

Figure 1 illustrates our approach for a published proband with five characteristic features of ataxia-pancytopenia

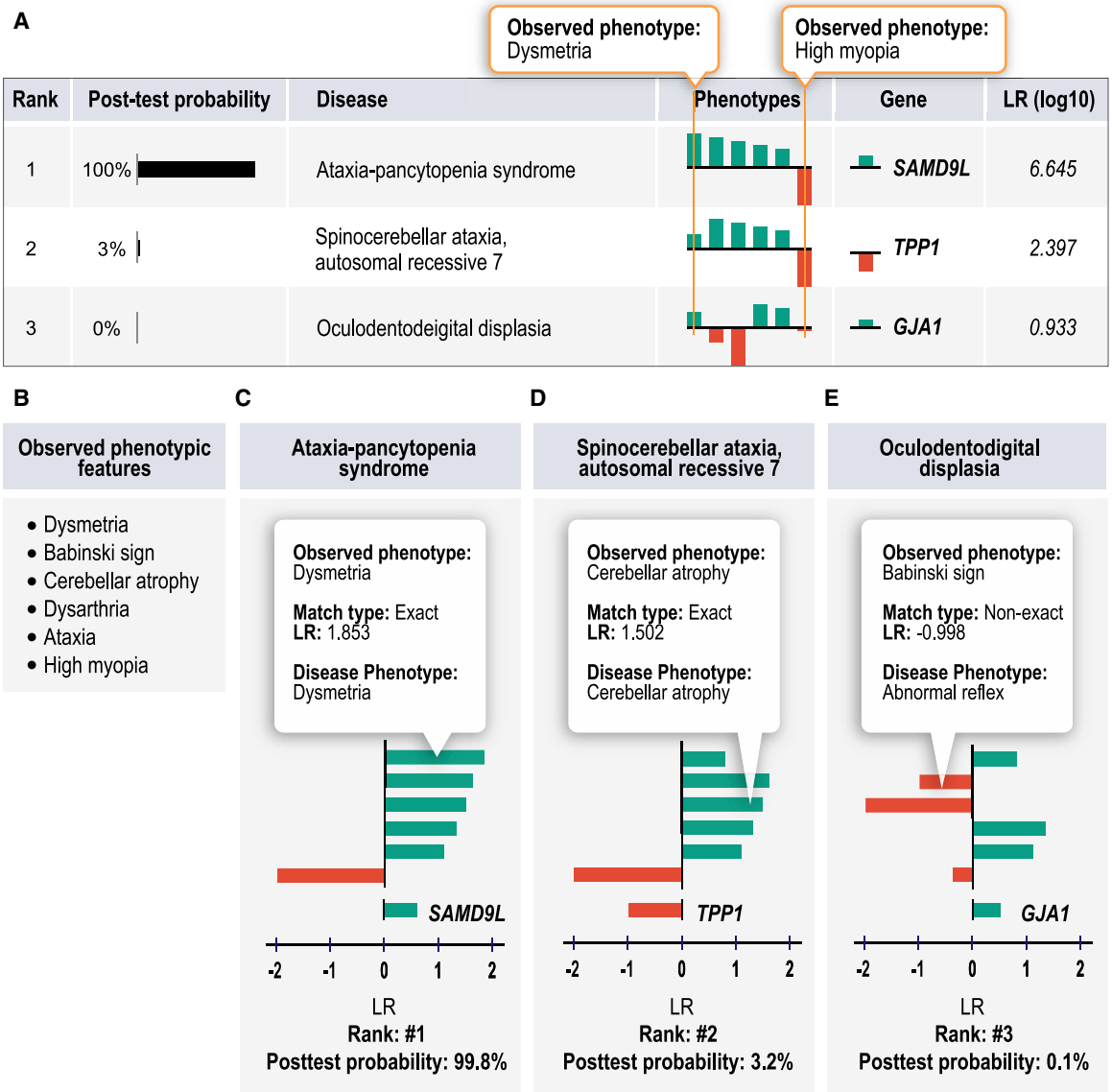

Figure 1. LIRICAL Evaluation of a Simulated Case of Ataxia-Pancytopenia Syndrome (ATXPC)
For each candidate diagnosis with an above-threshold posttest probability, LIRICAL shows the contribution of each phenotypic feature and of the genotype to the final diagnosis. In this case, the data were extracted from a published case report on an individual with ATXPC,[46] and an additional unrelated term (high myopia) was added to simulate the effect of noise.
(A) LIRICAL provides a table of the top candidates with the posttest probability and a sparkline view of the contributions of each HPO term and the relevant genotype.
(B) The observed HPO terms.
(C) The correct diagnosis, ATXPC, is ranked in first place because of a good phenotype match and a positive LR for the heterozygous genotype for the causative gene *SAMD9L*.
(D) The second candidate has many of the same phenotype matches, but the first query term, dysmetria, matches exactly with Ataxia-pancytopenia syndrome and only approximately with the second candidate, spinocerebellar ataxia, autosomal recessive 7.
(E) The third candidate has a posttest probability close to zero because it has more mismatching or poorly matching query terms.

syndrome (ATXPC; MIM: 159550): dysmetria, Babinski sign, cerebellar atrophy, dysarthria, and ataxia.[46] We additionally added the HPO term high myopia to simulate an unrelated (false-positive) finding that is not related to the underlying Mendelian disease. Exome sequencing was simulated in this example case by spiking a heterozygous variant in the causative gene for ATXPC, *SAMD9L*, into an otherwise "normal" VCF file. LIRICAL was then run on the combined phenotype and genotype data and ranked ATXPC first out of the 7,623 diseases in the HPO database. The graphical display of the results shown in Figure 1A indicates how much each feature contributed to the prediction. Figure 1D shows the second highest ranking candidate, spinocerebellar ataxia, autosomal recessive 7 (SCAR7). SCAR7 matches four of the five phenotypic features that ATXPC does. It scores lower because the

match to the term dysmetria was exact for ATXPC but in SCAR7 the closest match to dysmetria was ataxia, resulting in a lower LR (the HTML output of LIRICAL allows the user to browse the matching and approximate terms and their LRs by tool tips that appear when mousing over the bars that display the LR). The third candidate, oculodental dysplasia (MIM: 164200), has two additional mismatching HPO terms, Babinski sign and cerebellar atrophy, and is assigned a posttest probability of under 0.1%. LIRICAL thereby provides users both with an assessment of the degree to which any given phenotypic feature supports a diagnosis or argues against it, as well as an estimated posttest probability of the candidate diagnosis on the basis of the information provided. Users can remove terms deemed irrelevant (e.g., high myopia) and rerun the analysis. They can choose to concentrate detailed follow-up on candidate diagnoses with a high posttest probability.

LIRICAL Achieves State-of-the-Art Performance and Is Robust to Phenotypic and Genotypic Noise

We evaluated the performance of LIRICAL by using several different approaches. Many previous studies simulated cases by choosing a certain number of HPO terms at random to simulate a proband (e.g., choosing five terms at random from the 56 terms that annotate Marfan syndrome in the HPO database). Phenotypic noise is simulated by adding a certain number of HPO terms at random from all available annotations ("noise terms"). In some cases, imprecision of clinical data entry is simulated by replacing the randomly chosen disease terms by parent terms. If studies simulate genomic analysis, then additionally a published disease-associated variant would be spiked into an otherwise normal VCF file.[47–50] However, this kind of simulation can be criticized because randomly chosen terms are unlikely to resemble terms that would be chosen in a real clinical encounter. In a real clinical encounter, the clinician may or may not be able to describe phenotypic abnormalities with the greatest possible detail. For instance, a general practitioner may diagnose reduced visual acuity, but the precise abnormality, say Y-shaped cataract, may only be observable by an ophthalmologist. Therefore, in real-life situations, the different aspects of the phenotype of a proband may have been observed, recorded, or communicated at different levels of detail.

Our basic approach for this study was therefore to extract HPO terms and disease-causing variants from published case reports and to perform simulations with the original data as well as simulations in which varying types of phenotypic or genotypic noise were added. We tested the performance of LIRICAL by using a collection of 384 case reports derived from the literature and curated by using the GA4GH phenopacket format (Table 1; Web Resources). LIRICAL can be run with or without genetic data, and so we first compared it to Phenomizer, which exploits semantic similarity between query terms and diseases on the basis of clinical (but not genetic) data.[47] LIRICAL placed a total of 43.7% of cases in the top three ranks compared to 35.3% for Phenomizer (Figure S4).

We then compared LIRICAL to Exomiser, which has shown state-of-the-art performance against other algorithms.[49] Exomiser currently ranks disease genes (combining all diseases associated with any given gene), and so for this comparison, we recorded LIRICAL's rank by gene. LIRICAL placed the correct gene in the first ranks in 80.7% of cases, compared to 77.3% for Exomiser. The percentages for placing the correct gene in the top three ranks were 92.9% for LIRICAL and 92.2% for Exomiser (Figure 2B).

Diagnostic NGS data, including exome, genome, and gene-panel investigations, can be affected by many different kinds of noise.[15] The disease-causing variant may be missed, or in autosomal-recessive conditions, one of the two pathogenic alleles may fail to be detected. Phenotypic features unrelated to the Mendelian disease may be included in the analysis. On the other hand, phenotypic features associated with the disease may be observed or described imprecisely. LIRICAL was designed with a number of features that can help mitigate these kinds of noise.

We first compared the performance of both approaches in the presence of phenotypic noise (Figure 2A explains the obfuscations). Figure 2E shows the performance if two random HPO terms are added to each case to simulate noise. Figure 2F shows the effect of additionally replacing each of the original HPO terms with a parent term, and Figure 2G shows the effect of additionally replacing each original term with a grandparent term. The latter two experiments simulate the effect of two different degrees of imprecision in the description of the clinical data (e.g., not entering a term such as zonular cataract but instead entering its parent term, cataract, or even grandparent term, abnormality of the lens). It can be seen that LIRICAL's performance is better than Exomiser's on this dataset and that LIRICAL's performance degrades less in the presence of noise.

LIRICAL's genotype LR does not apply a hard filter to candidates whose genotype does not match the expected genotype for some disease. In exome and genome sequencing, structural variants and single-nucleotide or other small variants in GC-rich exons may be missed, which can lead to only one of two pathogenic alleles' being detected for an autosomal-recessive disease. LIRICAL will rate such a genotype less highly than a pathogenic biallelic genotype but will not filter out such candidates (Figure S5). We therefore compared the performance of LIRICAL and Exomiser on the 221 autosomal-recessive cases in our dataset. LIRICAL placed the correct candidate in first place in 84.6% of cases compared to 71.0% for Exomiser. If one of the two pathogenic alleles was removed, LIRICAL still placed the correct gene in first place in 62.0% of cases, compared to only 20.1% for Exomiser (Figures 2C and 2D). The performance of LIRICAL was slightly better in cases where at least one of the variants

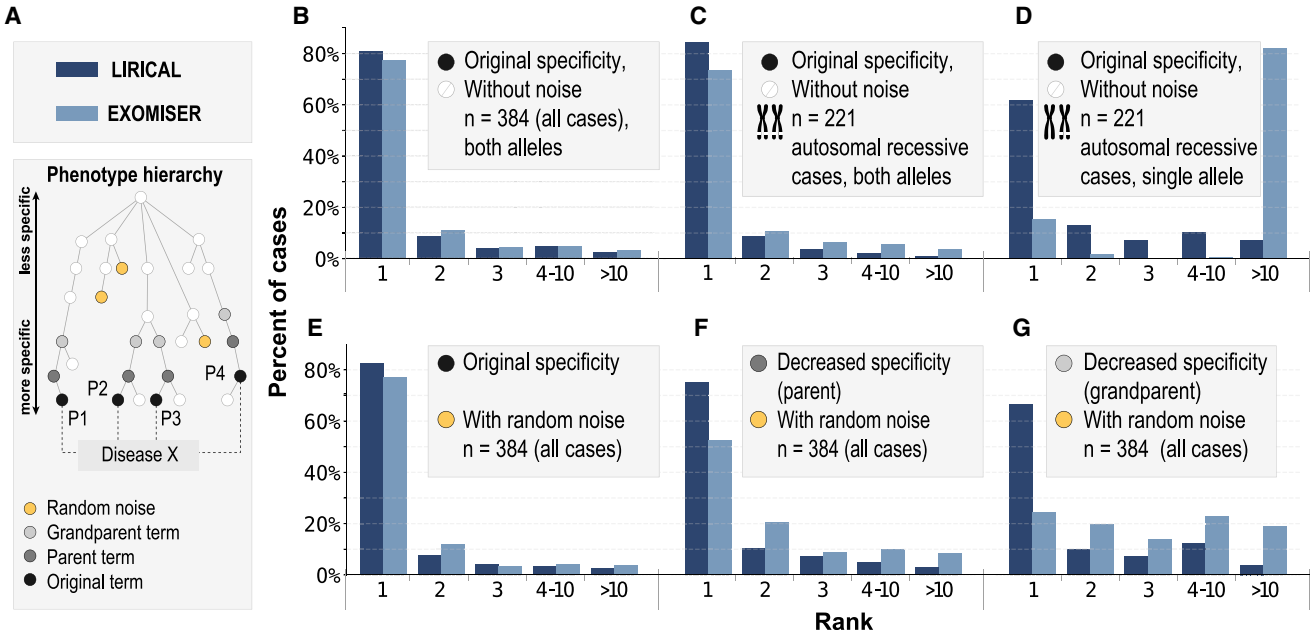

Figure 2. Evaluation of LIRICAL and Exomiser on 384 Case Studies

The case studies were formatted as phenopackets (Table 1), and the diagnostic process was simulated by spiking disease-causing variants into a VCF file, which was passed together with phenotype data to LIRICAL and Exomiser.

(A) Simulation approach. Random noise terms were added to some simulations, and in some cases, terms were replaced by their parent term or grandparent term to mimic imprecision in measuring or recording phenotypic abnormalities.

(B–G) Results of simulations are shown with the x axis showing the rank assigned by LIRICAL or Exomiser to the correct disease gene, and the y axis showing the percentage of cases in which the given rank was achieved. The following is shown: original data (B), performance on the subset of 221 autosomal-recessive cases (C), the same 221 autosomal-recessive cases in which one of the two pathogenic alleles was removed (D), two random ("noise") HPO terms added to each case (E), original terms replaced by a parent term and two noise terms added (F), and original terms replaced by a grandparent term and two noise terms added (G).

was listed as pathogenic by ClinVar for both AD and autosomal-recessive modes of inheritance (Figure S6).

LIRICAL ranked 259 of 384 (67.4%) cases at a posttest probability above 0.5, and 287 cases (74.7%) were above a posttest probability of 0.05. The overall rankings as well as the posttest probability were robust to the addition of noise, deteriorating only slightly when two random terms were added per case, somewhat more if terms were replaced by more general parent or even more general grandparent terms, and falling to a mean of only 29.4% if all pathogenic alleles were omitted and to 2.9% if all HPO terms were replaced by random terms (Figure 3). This suggests that LIRICAL assigns substantially mean lower posttest probabilities to candidate diseases for which an apparently pathogenic variant is identified by diagnostic NGS by chance but where there is no clinical match.

Finally, we examined 116 solved singleton cases from the 100,000 Genomes Project. All cases were singletons with single-sample VCF files available. The diagnoses came from 89 different genes across a wide spectrum of rare disease areas (cardiovascular, ciliopathies, dermatological, dysmorphic and congenital abnormalities, endocrine, hearing and ear, metabolic, neurology and neurodevelopmental, ophthalmological, renal and urinary tract, rheumatological, skeletal, tumor syndromes). LIRICAL placed the correct gene in first place in 60.3% of cases, compared to 64.6% for Exomiser, and placed the correct gene in the top five ranks in 88.8% compared to 87.1% for Exomiser (Figure 4). This is an impressive outcome, considering that Exomiser is already part of the 100,000 Genomes Project's diagnostic pipeline and was used as part of the decision-making process for 26 of the 115 diagnoses. Considering the 89 diagnoses where Exomiser was not utilized, Exomiser prioritized 57/89 (64.0%) in first place compared to 51/89 (57.3%) for LIRICAL.

Prioritization of Genes Associated with Multiple Diseases

Many Mendelian-disease-related genes are associated with more than one disease (for instance, mutations in *FBN1* are associated with both Marfan syndrome and geleophysic dysplasia). In contrast to Exomiser, LIRICAL ranks diseases rather than genes (for an example, see Figure 5). The by-disease ranking results for LIRICAL for the data in Figure 2B are shown in Figure S8.

Incorporation of ClinVar Data and Analysis of Excluded Phenotypic Abnormalities

LIRICAL uses several heuristic algorithms to account for some challenges in the prioritization of genomic data. For instance, genes such as *TTN* have a high population frequency of variants predicted computationally to be

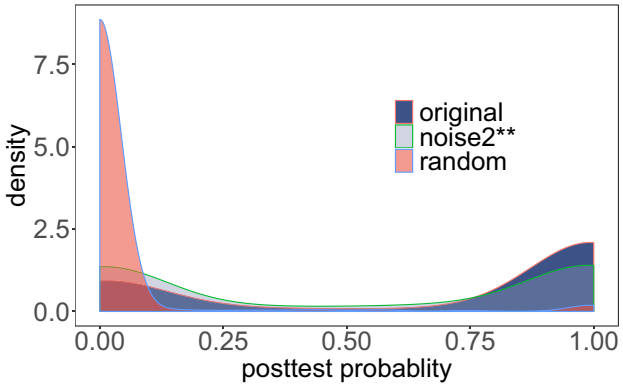

Figure 3. Posttest Probability
The posttest probability of the correct diagnosis was calculated for each of the 384 phenopacket case reports (original).
Densities are shown for the original data (original; mean posttest probability, pp, 67.4%.); noise2**, in which two random HPO terms were added and original terms were replaced by grandparent terms (mean pp, 50.3%); and random, in which all HPO terms were replaced by random terms (mean pp, 2.9%). Figure S7 shows results for other perturbations.

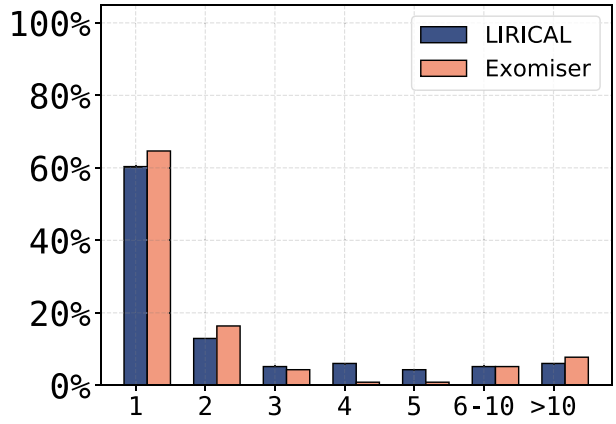

Figure 4. Performance of LIRICAL and Exomiser on 116 Solved Singleton Cases from the 100,000 Genomes Project
The x axis shows the rank assigned by LIRICAL or Exomiser to the correct disease gene. The y axis shows the percentage of cases in which the given rank was achieved.

pathogenic that are found in apparently healthy individuals. On the other hand, specific *TTN* variants are listed as pathogenic in ClinVar.[31] There is currently no approach that always correctly interprets pathogenicity of variants in such genes. In such cases, LIRICAL takes the approach of downweighting rare, predicted pathogenic variants without support in ClinVar, but heuristically assigns variants listed as pathogenic in ClinVar an LR score of 1,000. In a simulated case of *TTN*-related dilated cardiomyopathy, LIRICAL correctly ranks a known pathogenic variant in first place but ranks a rare variant that is computationally predicted to be pathogenic but is listed in ClinVar as uncertain only in eighth place (Figure S9).

In clinical practice, the differential diagnostic process can occasionally be empowered by identifying phenotypic abnormalities that a proband does not have. In medical genetics, many diseases share a number of phenotypic features but differ with respect to one characteristic feature that presents in one disease but never presents in others. Such a feature can be very important for the differential diagnosis. For instance, Loeys-Dietz syndrome 4 is not characterized by ectopia lentis, whereas the phenotypically similar disease Marfan syndrome is.[27] LIRICAL uses a heuristic to downweight candidate diagnoses by a factor of 1,000 if the candidate is explicitly annotated not to have a feature present in the query terms. Ten of the 380 phenopackets have excluded query terms (e.g., the individual does not have some HPO term) that support one candidate diagnosis (column 1 in Table S4) but speak against another (column 2 in the table). In all cases, the correct diagnosis via the negated annotations was 1, and the mean posttest probability was 98.9%. If the negated query term was omitted, the average rank was 1.3, and the mean posttest probability was 72.6% (Figure S10). Figure S11 shows an example of a differential diagnosis in which the omission of a negated term reduces the posttest probability of the correct diagnosis from 92.4% to 1.2% and changes the rank of the candidate from 1 to 2. To our knowledge, LIRICAL is the only HPO-based algorithm for genomic diagnostics that leverages information about excluded phenotypes in this way.

Simultaneous Analysis of Molecularly Elucidated and Idiopathic Diseases

Another feature of LIRICAL is a mode (–global) that ranks all candidates, including diseases whose molecular etiology is unknown as well as diseases with a known associated gene in which no pathogenic variants were identified. This is a harder prediction problem because there are more candidate diseases, but it can prioritize diseases that would be missed by conventional approaches. For example, Arima syndrome is an autosomal-recessive disease with no known disease-associated gene. LIRICAL prioritized it in first place in a simulated run in which some clinically similar diseases, such as Joubert syndrome, failed to achieve a good score (Figure S12). LIRICAL placed the correct diagnosis in first place in 24.5% of cases compared to 1.0% for Exomiser and placed the correct candidate in the top three ranks in 38.2% (1.0% for Exomiser). Overall, LIRICAL placed the correct candidate in the top ten ranks in roughly half of the cases (Figure S13).

Discussion

Clinical decision support systems and genomic diagnostics have rapidly been gaining importance in recent years. The interpretability of computational predictions is of utmost importance in clinical settings for clinicians to efficiently and correctly integrate computational analyses into medical workflows, and even accurate black-box algorithms might not be appropriate in clinical settings.[21,52,53] The LIRICAL algorithm presented here adapts the LR

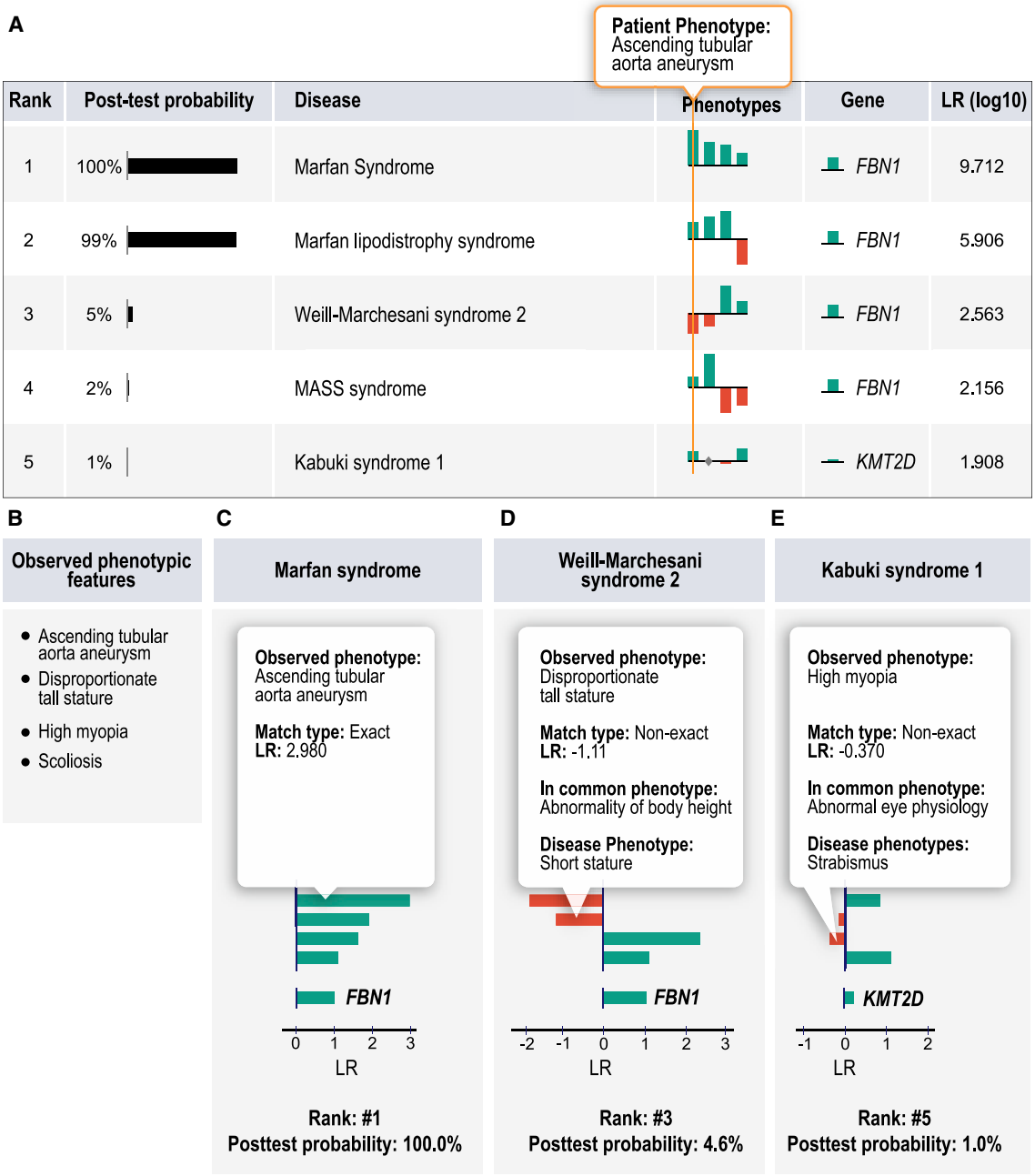

Figure 5. LIRICAL Evaluation of Simulated Case with a Pathogenic *FBN1* Variant
(A–E) Eight distinct diseases are associated with variants in *FBN1*. LIRICAL prioritizes each disease separately, and in this case correctly placed Marfan syndrome at rank #1. Three other *FBN1*-associated diseases were placed in ranks #2–#4 (A). Clinical and molecular data were simulated according to individual 1 in Cao et al.[51] The HPO terms are shown in panel (B). The graphic shows LIRICAL's summary table and three of the detailed LR plots for the candidates at ranks #1 (C), #3 (D), and #5 (E).

framework that is widely used in the interpretation of clinical laboratory results.[22,54,55] To the best of our knowledge, the LR framework has not previously been used to support phenotype-driven genomic diagnostics. LIRICAL provides predictions of rare-disease diagnoses whose accuracy is at par with that of previous state-of-the-art approaches, such as Exomiser.[29] LIRICAL exhibits substantially better performance in the face of phenotypic and genotypic noise. Additionally, it provides an estimated posttest probability of each candidate diagnosis and allows clinicians to evaluate the contribution of each individual phenotypic abnormality to each candidate diagnosis.

An LR indicates how many times more or less likely individuals with the disease are to have that particular result than are individuals without the disease. An LR greater than one indicates that the result of the test is associated with the presence of the disease being investigated, whereas an LR less than one indicates the absence of the disease. The more the value of the LR deviates from one, the stronger the evidence is for the presence or absence of disease.[43] In

practice, the posttest probability can be used as an estimate of the quality of any diagnosis. The mean posttest probability estimated for the candidate at rank one for randomized data was close to zero, whereas the posttest probability of the correct diagnosis was about 67% for the case reports (Figure 3). In some cases, however, the correct candidate was placed at rank one but received a low posttest probability. Future improvements in the quality and comprehensiveness of HPO annotations as well as in the computational assessment of variants might lead to an improved ability of LIRICAL to estimate posttest probabilities.

LIRICAL can analyze an exome in less than a minute on a typical laptop computer. We identified 14 other tools for phenotype-driven analysis of diagnostic exome or genome data. None of these tools was both up to date and available for execution on the command line, which would have enabled testing of the total of 1,978 original or obfuscated cases from the phenopackets and the 116 cases from the 100,000 Genomes Project (Table S5).

In addition to having a performance that is comparable to that of other state-of-the-art tools, such as Exomiser, LIRICAL provides users with interpretable results that can be used to guide clinical actions. For instance, large-scale disease-sequencing projects, such as the 100,000 Genomes Project, often have hundreds or thousands of unsolved cases. LIRICAL can be run on collections of unsolved cases, and the posttest probability of the highest ranked candidates could be used as a criterion to decide whether to subject a case to detailed reanalysis.

LIRICAL's assessment of the contribution of individual phenotypic abnormalities can also be useful in many ways. For instance, in practice, individuals with genetic diseases may present with a mix of signs and symptoms that are related to an underlying Mendelian disorder and may also have unrelated (coincidental) findings. If a core set of phenotypes and a genotype strongly support a candidate diagnosis but some features do not, clinicians might consider whether alternate explanations for the noncontributory features are plausible according to their clinical judgment. For instance, features such as myopia, scoliosis, and gastresophageal reflux are relatively common in the general population and might therefore occur in persons with genetic disease as coincidental findings. Clinical judgment would be necessary to evaluate each term. For instance, myopia (short-sightedness) is relatively common in young adults, but the presence of high myopia in a toddler is more likely to be a clinical finding that is important for the differential diagnostic workup.

LIRICAL takes as input a list of HPO terms and can be run with or without an associated VCF file with genetic variants. The Java implementation of LIRICAL presented here assumes an equal pretest probability for each of the diseases under consideration (e.g., $(1/7,596)$ for the 7,596 diseases currently represented in the HPO database). This is a reasonable approach to the analysis of exomes in a setting such as the 100,000 Genomes Project where we speculate that rarer genetic diseases are more likely to be analyzed than common, more easily recognized genetic diseases. However, in other settings, LIRICAL could be used with other values for the pretest probability. For instance, in general care settings, the rare-disease prevalence data from Orphanet could be used.[56]

Limitations

Similar to the Naive Bayes approach, LIRICAL makes the assumption that the individual (phenotypic) features are independent of each other; this is called "naive" because it is almost never true. However, in practice, Naive Bayes and LIRICAL perform well on real data. In the future, the LIRICAL algorithm could be extended to model the dependencies in the data by defining compound probability distributions. For instance, what is the probability of observing a set of abnormalities of the skeleton given that a certain diagnosis is present or not? Speculatively, this could further improve the performance of LIRICAL, but it would require data about co-occurrences of phenotypic features that are currently not generally available.

Several of LIRICAL's features depend on the underlying biocurated data. Currently, the HPO database contains 10,756 annotations of 2,321 diseases with explicit frequency data, meaning that most annotations have an unknown frequency (the LIRICAL algorithm uses the default frequency of 100% in these cases). Therefore, deeper and more detailed biocuration will be required to take advantage of LIRICAL's ability to use frequencies to calculate the LR.

Data and Code Availability

LIRICAL is implemented as a stand-alone Java desktop application that can be installed in less than an hour. LIRICAL is freely available for academic use, and source code can be downloaded from https://github.com/TheJacksonLaboratory/LIRICAL. The 384 phenopackets generated for this work are available via zenodo (https://zenodo.org/record/3905420).

Supplemental Data

Supplemental Data can be found online at https://doi.org/10.1016/j.ajhg.2020.06.021.

Acknowledgments

This work was supported by internal funding of the Jackson Laboratory. Additional support was provided by the National Institutes of Health (NIH) Office of the Director (1R24OD011883). The UNC Biocuration Core was supported by NHGRI U41HG009650.

Declaration of Interests

P.N.R. has filed a patent application based on this work.

Received: January 25, 2020
Accepted: June 26, 2020
Published: August 4, 2020

Web Resources

ClinVar, https://www.ncbi.nlm.nih.gov/clinvar/
Global Alliance for Genomics and Health (GA4GH) Phenopacket format, https://github.com/phenopackets/phenopacket-schema
Human Phenotype Ontology, https://hpo.jax.org/app/
LIRICAL, https://github.com/TheJacksonLaboratory/LIRICAL
LIRICAL documentation, https://lirical.readthedocs.io/
OMIM, https://www.omim.org

References

1. Sifrim, A., Popovic, D., Tranchevent, L.-C., Ardeshirdavani, A., Sakai, R., Konings, P., Vermeesch, J.R., Aerts, J., De Moor, B., and Moreau, Y. (2013). eXtasy: variant prioritization by genomic data fusion. Nat. Methods *10*, 1083–1084.
2. Singleton, M.V., Guthery, S.L., Voelkerding, K.V., Chen, K., Kennedy, B., Margraf, R.L., Durtschi, J., Eilbeck, K., Reese, M.G., Jorde, L.B., et al. (2014). Phevor combines multiple biomedical ontologies for accurate identification of disease-causing alleles in single individuals and small nuclear families. Am. J. Hum. Genet. *94*, 599–610.
3. Javed, A., Agrawal, S., and Ng, P.C. (2014). Phen-Gen: combining phenotype and genotype to analyze rare disorders. Nat. Methods *11*, 935–937.
4. Smedley, D., Jacobsen, J.O., Jäger, M., Köhler, S., Holtgrewe, M., Schubach, M., Siragusa, E., Zemojtel, T., Buske, O.J., Washington, N.L., et al. (2015). Next-generation diagnostics and disease-gene discovery with the Exomiser. Nat. Protoc. *10*, 2004–2015.
5. Miller, N.A., Farrow, E.G., Gibson, M., Willig, L.K., Twist, G., Yoo, B., Marrs, T., Corder, S., Krivohlavek, L., Walter, A., et al. (2015). A 26-hour system of highly sensitive whole genome sequencing for emergency management of genetic diseases. Genome Med. *7*, 100.
6. Yang, H., Robinson, P.N., and Wang, K. (2015). Phenolyzer: phenotype-based prioritization of candidate genes for human diseases. Nat. Methods *12*, 841–843.
7. James, R.A., Campbell, I.M., Chen, E.S., Boone, P.M., Rao, M.A., Bainbridge, M.N., Lupski, J.R., Yang, Y., Eng, C.M., Posey, J.E., and Shaw, C.A. (2016). A visual and curatorial approach to clinical variant prioritization and disease gene discovery in genome-wide diagnostics. Genome Med. *8*, 13.
8. Godard, P., and Page, M. (2016). PCAN: phenotype consensus analysis to support disease-gene association. BMC Bioinformatics *17*, 518.
9. Stelzer, G., Plaschkes, I., Oz-Levi, D., Alkelai, A., Olender, T., Zimmerman, S., Twik, M., Belinky, F., Fishilevich, S., Nudel, R., et al. (2016). VarElect: the phenotype-based variation prioritizer of the GeneCards Suite. BMC Genomics *17* (*Suppl 2*), 444.
10. Krämer, A., Shah, S., Rebres, R.A., Tang, S., and Richards, D.R. (2017). Leveraging network analytics to infer patient syndrome and identify causal genes in rare disease cases. BMC Genomics *18* (*Suppl 5*), 551.
11. Lionel, A.C., Costain, G., Monfared, N., Walker, S., Reuter, M.S., Hosseini, S.M., Thiruvahindrapuram, B., Merico, D., Jobling, R., Nalpathamkalam, T., et al. (2018). Improved diagnostic yield compared with targeted gene sequencing panels suggests a role for whole-genome sequencing as a first-tier genetic test. Genet. Med. *20*, 435–443.
12. Rao, A., Vg, S., Joseph, T., Kotte, S., Sivadasan, N., and Srinivasan, R. (2018). Phenotype-driven gene prioritization for rare diseases using graph convolution on heterogeneous networks. BMC Med. Genomics *11*, 57.
13. Köhler, S., Carmody, L., Vasilevsky, N., Jacobsen, J.O.B., Danis, D., Gourdine, J.-P., Gargano, M., Harris, N.L., Matentzoglu, N., McMurry, J.A., et al. (2019). Expansion of the Human Phenotype Ontology (HPO) knowledge base and resources. Nucleic Acids Res. *47* (D1), D1018–D1027.
14. Bergmann, C., Fliegauf, M., Brüchle, N.O., Frank, V., Olbrich, H., Kirschner, J., Schermer, B., Schmedding, I., Kispert, A., Kränzlin, B., et al. (2008). Loss of nephrocystin-3 function can cause embryonic lethality, Meckel-Gruber-like syndrome, situs inversus, and renal-hepatic-pancreatic dysplasia. Am. J. Hum. Genet. *82*, 959–970.
15. Robinson, P.N., Piro, R., and Jäger, M. (2017). Computational Exome and Genome Analysis. (Chapman & Hall/CRC Mathematical and Computational Biology).
16. Smedley, D., and Robinson, P.N. (2015). Phenotype-driven strategies for exome prioritization of human Mendelian disease genes. Genome Med. *7*, 81.
17. Sawyer, S.L., Hartley, T., Dyment, D.A., Beaulieu, C.L., Schwartzentruber, J., Smith, A., Bedford, H.M., Bernard, G., Bernier, F.P., Brais, B., et al.; FORGE Canada Consortium; and Care4Rare Canada Consortium (2016). Utility of whole-exome sequencing for those near the end of the diagnostic odyssey: time to address gaps in care. Clin. Genet. *89*, 275–284.
18. Tan, T.Y., Dillon, O.J., Stark, Z., Schofield, D., Alam, K., Shrestha, R., Chong, B., Phelan, D., Brett, G.R., Creed, E., et al. (2017). Diagnostic impact and cost-effectiveness of whole-exome sequencing for ambulant children with suspected monogenic conditions. JAMA Pediatr. *171*, 855–862.
19. Dragojlovic, N., Elliott, A.M., Adam, S., van Karnebeek, C., Lehman, A., Mwenifumbo, J.C., Nelson, T.N., du Souich, C., Friedman, J.M., and Lynd, L.D. (2018). The cost and diagnostic yield of exome sequencing for children with suspected genetic disorders: a benchmarking study. Genet. Med. *20*, 1013–1021.
20. Wright, C.F., FitzPatrick, D.R., and Firth, H.V. (2018). Paediatric genomics: diagnosing rare disease in children. Nat. Rev. Genet. *19*, 253–268.
21. Rudin, C. (2019). Stop explaining black box machine learning models for high stakes decisions and use interpretable models instead. Nat. Mach. Intell. *1*, 206–215.
22. Albert, A. (1982). On the use and computation of likelihood ratios in clinical chemistry. Clin. Chem. *28*, 1113–1119.
23. Robinson, P.N., Köhler, S., Bauer, S., Seelow, D., Horn, D., and Mundlos, S. (2008). The Human Phenotype Ontology: a tool for annotating and analyzing human hereditary disease. Am. J. Hum. Genet. *83*, 610–615.
24. Köhler, S., Doelken, S.C., Mungall, C.J., Bauer, S., Firth, H.V., Bailleul-Forestier, I., Black, G.C.M., Brown, D.L., Brudno, M., Campbell, J., et al. (2014). The Human Phenotype Ontology project: linking molecular biology and disease through phenotype data. Nucleic Acids Res. *42*, D966–D974.
25. Köhler, S., Vasilevsky, N.A., Engelstad, M., Foster, E., McMurry, J., Aymé, S., Baynam, G., Bello, S.M., Boerkoel, C.F., Boycott, K.M., et al. (2017). The Human Phenotype Ontology in 2017. Nucleic Acids Res. *45* (D1), D865–D876.

26. Robinson, P.N., and Bauer, S. (2011). Introduction to Biol.-Ontologies. (Chapman & Hall/CRC Mathematical and Computational Biology).
27. von Kodolitsch, Y., and Robinson, P.N. (2007). Marfan syndrome: an update of genetics, medical and surgical management. Heart *93*, 755–760.
28. Sheikhzadeh, S., Brockstaedt, L., Habermann, C.R., Sondermann, C., Bannas, P., Mir, T.S., Staebler, A., Seidel, H., Keyser, B., Arslan-Kirchner, M., et al. (2014). Dural ectasia in Loeys-Dietz syndrome: comprehensive study of 30 patients with a TGFBR1 or TGFBR2 mutation. Clin. Genet. *86*, 545–551.
29. Robinson, P.N., Köhler, S., Oellrich, A., Wang, K., Mungall, C.J., Lewis, S.E., Washington, N., Bauer, S., Seelow, D., Krawitz, P., et al.; Sanger Mouse Genetics Project (2014). Improved exome prioritization of disease genes through cross-species phenotype comparison. Genome Res. *24*, 340–348.
30. Lek, M., Karczewski, K.J., Minikel, E.V., Samocha, K.E., Banks, E., Fennell, T., O'Donnell-Luria, A.H., Ware, J.S., Hill, A.J., Cummings, B.B., et al.; Exome Aggregation Consortium (2016). Analysis of protein-coding genetic variation in 60,706 humans. Nature *536*, 285–291.
31. Landrum, M.J., Lee, J.M., Benson, M., Brown, G.R., Chao, C., Chitipiralla, S., Gu, B., Hart, J., Hoffman, D., Jang, W., et al. (2018). ClinVar: improving access to variant interpretations and supporting evidence. Nucleic Acids Res. *46* (D1), D1062–D1067.
32. Fuentes Fajardo, K.V., Adams, D., Mason, C.E., Sincan, M., Tifft, C., Toro, C., Boerkoel, C.F., Gahl, W., Markello, T.; and NISC Comparative Sequencing Program (2012). Detecting false-positive signals in exome sequencing. Hum. Mutat. *33*, 609–613.
33. Petrovski, S., Wang, Q., Heinzen, E.L., Allen, A.S., and Goldstein, D.B. (2013). Genic intolerance to functional variation and the interpretation of personal genomes. PLoS Genet. *9*, e1003709.
34. Feller, W. (1968). An Introduction to Probability Theory and Its Applications, *Volume 1* (Wiley).
35. Richards, S., Aziz, N., Bale, S., Bick, D., Das, S., Gastier-Foster, J., Grody, W.W., Hegde, M., Lyon, E., Spector, E., et al. (2015). Standards and guidelines for the interpretation of sequence variants: a joint consensus recommendation of the American College of Medical Genetics and Genomics and the Association for Molecular Pathology. Genet. Med. *17*, 405–424.
36. Amberger, J.S., Bocchini, C.A., Scott, A.F., and Hamosh, A. (2019). OMIM.org: leveraging knowledge across phenotype-gene relationships. Nucleic Acids Res. *47* (D1), D1038–D1043.
37. Maiella, S., Olry, A., Hanauer, M., Lanneau, V., Lourghi, H., Donadille, B., Rodwell, C., Köhler, S., Seelow, D., Jupp, S., et al. (2018). Harmonising phenomics information for a better interoperability in the rare disease field. Eur. J. Med. Genet. *61*, 706–714.
38. Rath, A., Olry, A., Dhombres, F., Brandt, M.M., Urbero, B., and Ayme, S. (2012). Representation of rare diseases in health information systems: the Orphanet approach to serve a wide range of end users. Hum. Mutat. *33*, 803–808.
39. Freeman, P.J., Hart, R.K., Gretton, L.J., Brookes, A.J., and Dalgleish, R. (2018). VariantValidator: Accurate validation, mapping, and formatting of sequence variation descriptions. Hum. Mutat. *39*, 61–68.
40. Zook, J.M., Catoe, D., McDaniel, J., Vang, L., Spies, N., Sidow, A., Weng, Z., Liu, Y., Mason, C.E., Alexander, N., et al. (2016). Extensive sequencing of seven human genomes to characterize benchmark reference materials. Sci. Data *3*, 160025.
41. Danecek, P., and McCarthy, S.A. (2017). BCFtools/csq: haplotype-aware variant consequences. Bioinformatics *33*, 2037–2039.
42. Pauker, S.G., and Kassirer, J.P. (1975). Therapeutic decision making: a cost-benefit analysis. N. Engl. J. Med. *293*, 229–234.
43. Deeks, J.J., and Altman, D.G. (2004). Diagnostic tests 4: likelihood ratios. BMJ *329*, 168–169.
44. Santoro, C., Bernardo, P., Coppola, A., Pugliese, U., Cirillo, M., Giugliano, T., Piluso, G., Cinalli, G., Striano, S., Bravaccio, C., and Perrotta, S. (2018). Seizures in children with neurofibromatosis type 1: is neurofibromatosis type 1 enough? Ital. J. Pediatr. *44*, 41.
45. McGaughran, J.M., Harris, D.I., Donnai, D., Teare, D., MacLeod, R., Westerbeek, R., Kingston, H., Super, M., Harris, R., and Evans, D.G. (1999). A clinical study of type 1 neurofibromatosis in north west England. J. Med. Genet. *36*, 197–203.
46. Chen, D.-H., Below, J.E., Shimamura, A., Keel, S.B., Matsushita, M., Wolff, J., Sul, Y., Bonkowski, E., Castella, M., Taniguchi, T., et al. (2016). Ataxia-pancytopenia syndrome is caused by missense mutations in SAMD9L. Am. J. Hum. Genet. *98*, 1146–1158.
47. Köhler, S., Schulz, M.H., Krawitz, P., Bauer, S., Dölken, S., Ott, C.E., Mundlos, C., Horn, D., Mundlos, S., and Robinson, P.N. (2009). Clinical diagnostics in human genetics with semantic similarity searches in ontologies. Am. J. Hum. Genet. *85*, 457–464.
48. Zemojtel, T., Köhler, S., Mackenroth, L., Jäger, M., Hecht, J., Krawitz, P., Graul-Neumann, L., Doelken, S., Ehmke, N., Spielmann, M., et al. (2014). Effective diagnosis of genetic disease by computational phenotype analysis of the disease-associated genome. Sci. Transl. Med. *6*, 252ra123.
49. Ebiki, M., Okazaki, T., Kai, M., Adachi, K., and Nanba, E. (2019). Comparison of causative variant prioritization tools using next-generation sequencing data in Japanese patients with Mendelian disorders. Yonago Acta Med. *62*, 244–252.
50. Li, Z., Zhang, F., Wang, Y., Qiu, Y., Wu, Y., Lu, Y., Yang, L., Qu, W.J., Wang, H., Zhou, W., and Tian, W. (2019). PhenoPro: a novel toolkit for assisting in the diagnosis of Mendelian disease. Bioinformatics *35*, 3559–3566.
51. Cao, Y., Tan, H., Li, Z., Linpeng, S., Long, X., Liang, D., and Wu, L. (2018). Three novel mutations in FBN1 and TGFBR2 in patients with the syndromic form of thoracic aortic aneurysms and dissections. Int. Heart J. *59*, 1059–1068.
52. Billiet, L., Van Huffel, S., and Van Belle, V. (2018). Interval coded scoring: a toolbox for interpretable scoring systems. PeerJ Comput. Sci. *4*, e150.
53. Yu, K.-H., Beam, A.L., and Kohane, I.S. (2018). Artificial intelligence in healthcare. Nat. Biomed. Eng. *2*, 719–731.
54. Grimes, D.A., and Schulz, K.F. (2005). Refining clinical diagnosis with likelihood ratios. Lancet *365*, 1500–1505.
55. Morgan, A.A., Chen, R., and Butte, A.J. (2010). Likelihood ratios for genome medicine. Genome Med. *2*, 30.
56. Nguengang Wakap, S., Lambert, D.M., Olry, A., Rodwell, C., Gueydan, C., Lanneau, V., Murphy, D., Le Cam, Y., and Rath, A. (2019). Estimating cumulative point prevalence of rare diseases: analysis of the Orphanet database. Eur. J. Hum. Genet. *28*, 165–173.

The American Journal of Human Genetics, Volume *107*

Supplemental Data

Interpretable Clinical Genomics with a Likelihood Ratio Paradigm

Peter N. Robinson, Vida Ravanmehr, Julius O.B. Jacobsen, Daniel Danis, Xingmin Aaron Zhang, Leigh C. Carmody, Michael A. Gargano, Courtney L. Thaxton, UNC Biocuration Core, Guy Karlebach, Justin Reese, Manuel Holtgrewe, Sebastian Köhler, Julie A. McMurry, Melissa A. Haendel, and Damian Smedley

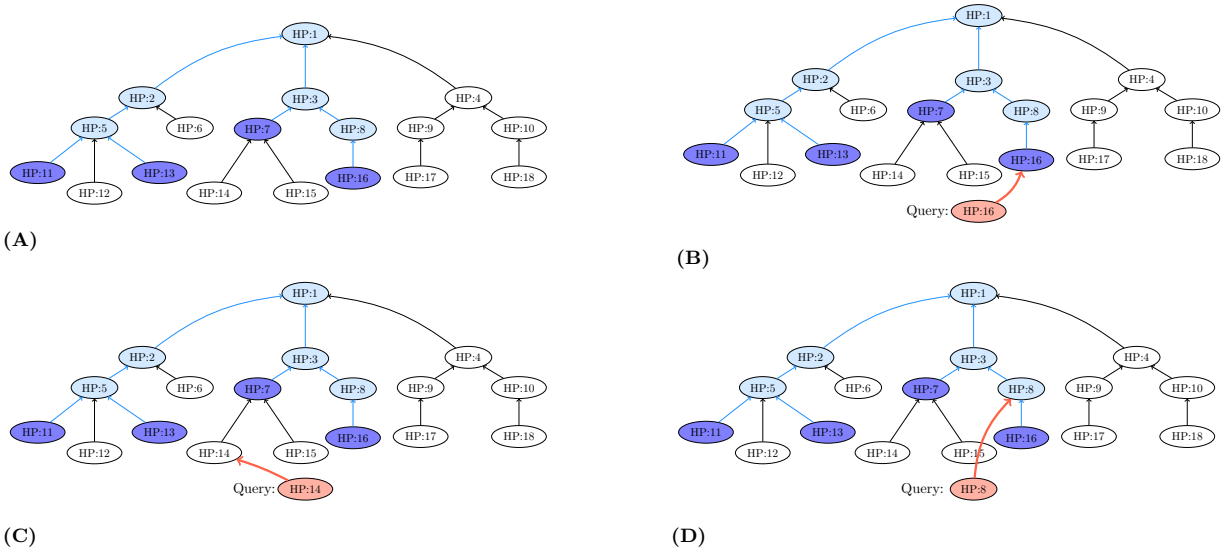

Figure S1. Calculating the likelihood ratios for phenotypes. **(A)** We will explain how the likelihood ratios (LR) for phenotypes are calculated using the example ontology shown here. The ontology contains 17 terms. For a certain disease, which we will call $\mathcal{D}$, four of the terms are directly annotated (HP:7, HP:11, HP:13, and HP:16, shown in dark blue). Because of the propagation of annotations, each of the ancestors of these terms is implicitly annotated to $\mathcal{D}$ as well (the terms are shown in light blue, and the edges encoding this inheritance are also shown in light blue). For instance, if HP:15 refers to `Nuclear cataract`, HP:8 refers to `Cataract`, and HP:3 refers to `Abnormal lens morphology`, then if we annotate disease $\mathcal{D}$ to `Nuclear cataract`, then we are also stating that the disease is characterized by `Cataract` and by `Abnormal lens morphology`. The term HP:1 is the root of this ontology (comparable to `Phenotypic abnormality` in the full HPO); **(B)** In this case a query term matches one of the directly annotated terms exactly. Then probability of observing HP:16 in an individual with $\mathcal{D}$ is simply the frequency of HP:16 in $\mathcal{D}$, or $P(h_{16}|\mathcal{D}) = f_{16}^{\mathcal{D}}$; **(C)** In this case, the query (HP:14) term matches a descendent of HP:7. HP:14 is not itself annotated to $\mathcal{D}$. In this case, we assume that the direct annotation (HP:7) is equally likely to correspond to an of its k subterms. If we assume that all individuals with disease $\mathcal{D}$ have the phenotypic feature represented by HP:7, then the frequency is 100%, i.e., $f_7^{\mathcal{D}} = 1.0$. We therefore divide this frequency by k. In this case, HP:7 has two descendents and $k = 2$, and therefore $P(h_{14}|\mathcal{D}) = \frac{f_7^{\mathcal{D}}}{2} = 0.5$; **(D)** Here, the query is to HP:8, an ancestor of a term that is directly annotated to $\mathcal{D}$. Because of annotation propagation, the probability of observing HP:8 in individuals with this disease is equivalent to the probability of observing HP:16, viz., $P(h_8|\mathcal{D}) = f_{16}^{\mathcal{D}}$.

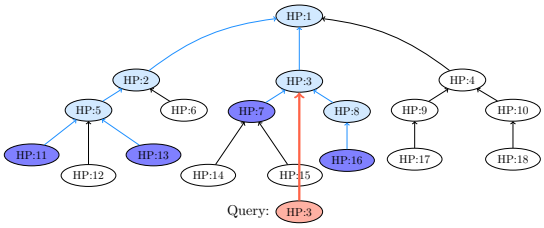

(E)

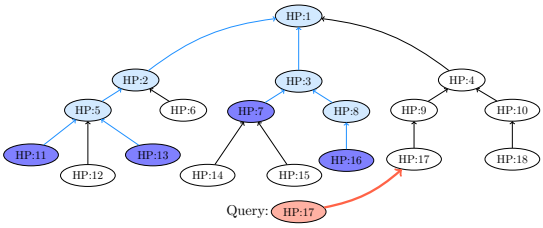

(F)

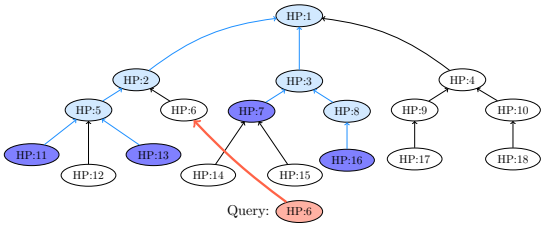

(G)

Figure S1. Calculating the likelihood ratios for phenotypes (continued). **(E)** HP:3 is an ancestor of two terms used to annotate $\mathcal{D}$. Here the maximum probability of HP:7 and HP:16 is taken, i.e., $P(h_3|\mathcal{D}) = \max(f_7^{\mathcal{D}}, f_{16}^{\mathcal{D}})$; **(F and G)** In this case, the query term is not directly annotated in the disease and is not a subclass of a disease term, nor is a disease term a subclass of the query term. Following the graph, the query term and some disease annotation have a common ancestor. This common ancestor can be a root term (**F**) or a non-root term (**G**). If their common ancestor is at the root, then the query does not affect an organ that is affected by the disease. An arbitrary small likelihood ratio of $\frac{1}{100}$ is assigned in this case. If there is a common ancestor below the root (h_{ca}), then the query term affects the same organ as the disease annotation without being a closely matched feature. In this case, we model the probability as being related to the overall frequency of the feature in the HPO corpus, but set the probability to be a minimum of $\frac{1}{100}$ to avoid an overly large influence of very rare features.

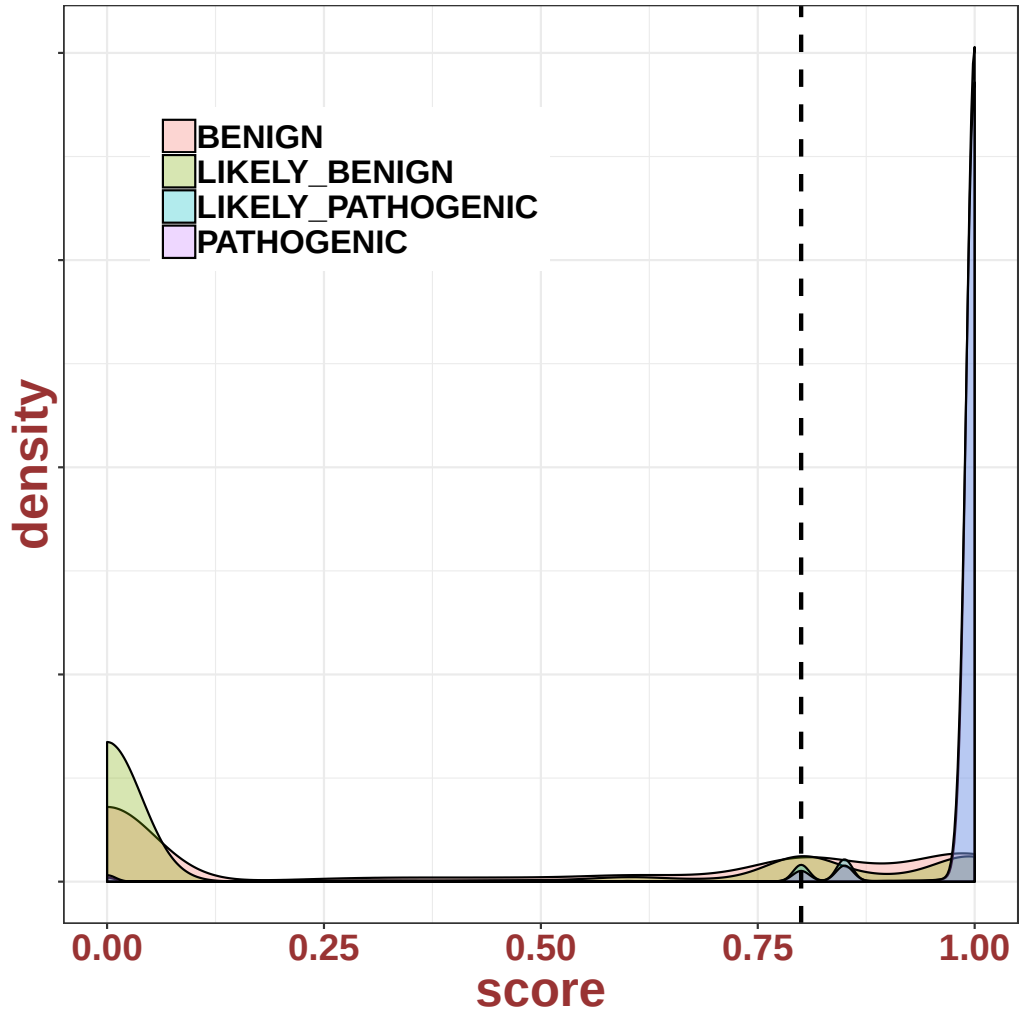

Figure S2. The Exomiser predicted pathogenicity score was calculated for each variant in ClinVar whose genomic position was precisely specified as nucleotide positions (these tend to be single-nucleotide variants or variants encompassing a small number of nucleotides rather than structural variants). A total of 160,714 such variants were available for analysis in the Exomiser data distribution version 12.1.0. The were 16,499 `benign` variants (10.3%), 64,123 `likely benign` variants (39.9%), 27,830 `likely pathogenic` variants (17.3%), and 52,262 `pathogenic` variants (32.5%). For the purpose of this analysis, the category `likely benign or benign` was assigned to `likely benign`, and `likely pathogenic or pathogenic` was assigned to `likely pathogenic`. In this work, a threshold pathogenicity score of 0.8 was chosen. The percentages of variants with an Exomiser score of at least 0.8 was: `benign`: 36.1%, `likely benign`: 26.5%, `likely pathogenic`: 99.3%, and `pathogenic`: 98.9%. The analysis was performed using the hg19 data. Similar results were obtained for hg38.

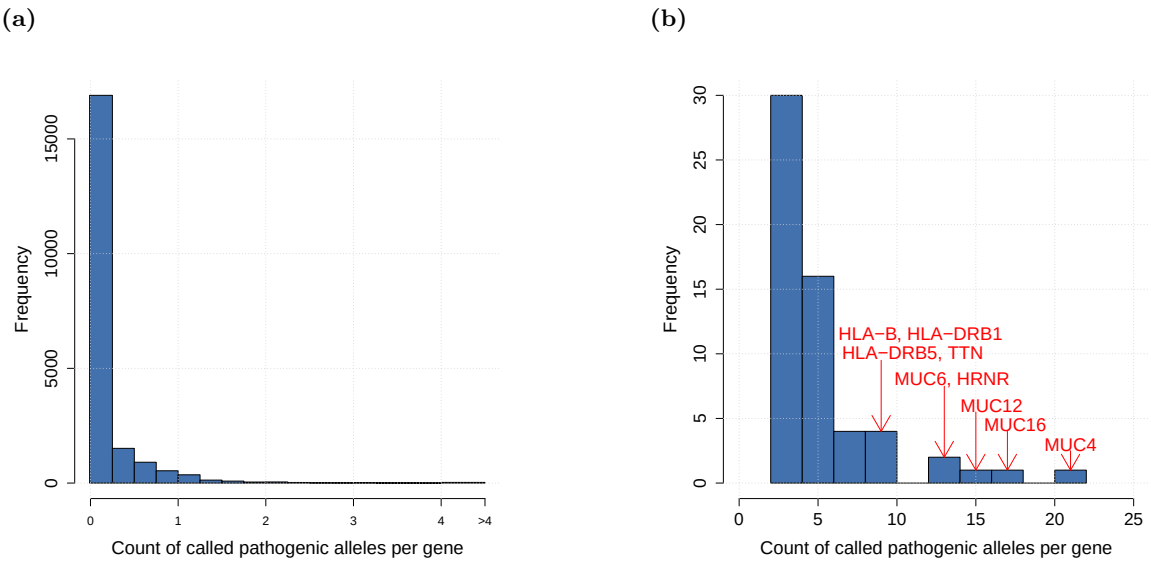

Figure S3. Frequencies of called pathogenic variants per gene. The frequencies of variants whose predicted pathogenicity score was 0.8 or higher was summed for each of 20,632 protein-coding genes and the count (frequency) of genes is plotted. Data are derived from the hg19 gnomAD dataset. Similar results were obtained for hg38. **(a)** An overview of the entire distribution. **(b)** Counts are shown for the 59 genes with counts above 3. Gene symbols are shown for all genes with counts above 8.

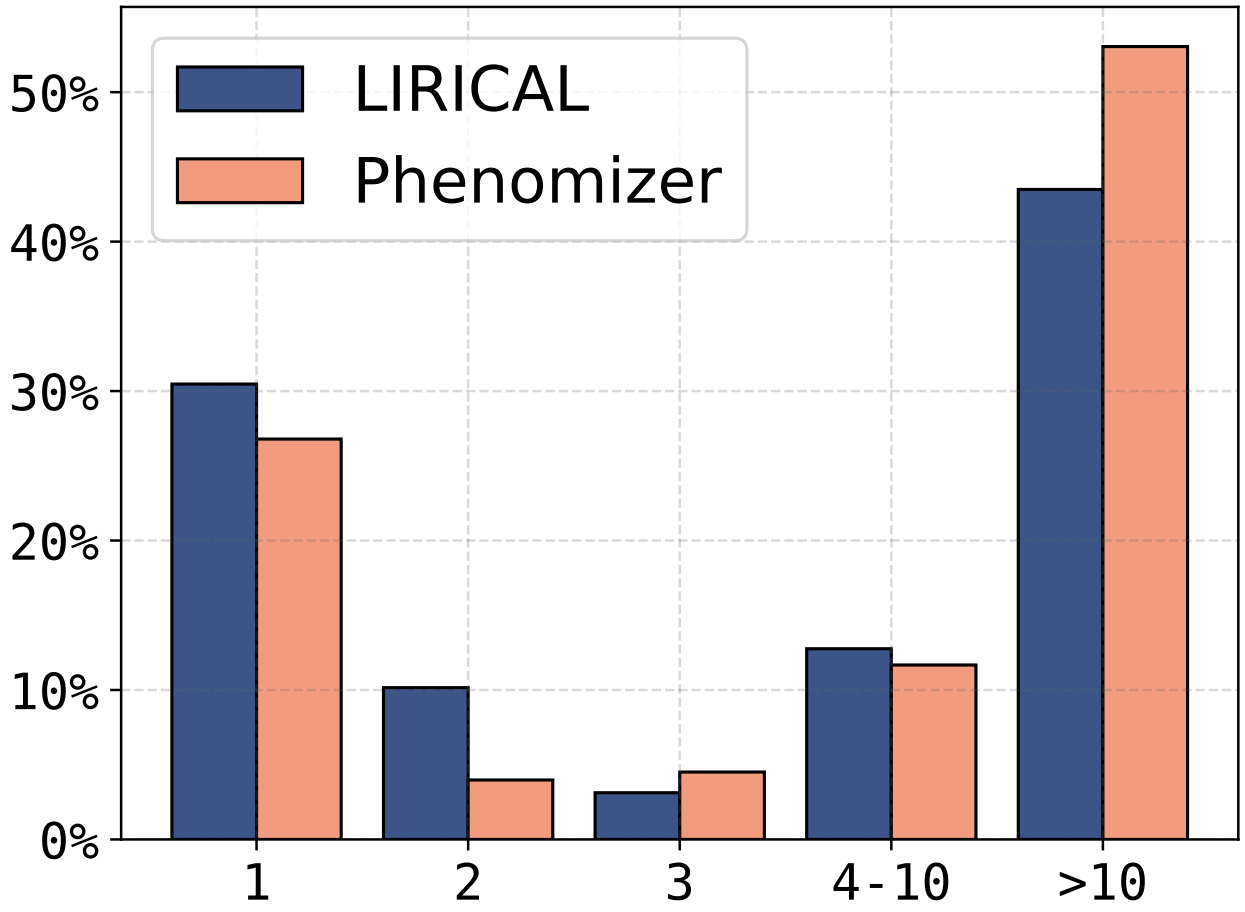

Figure S4. Comparison of LIRICAL and Phenomizer. The performance of LIRICAL (phenotype-only mode) was compared with that of Phenomizer [1] on the dataset of 384 Phenopackets (Table S2). For this analysis, the genetic information was not used, because Phenomizer is not able to use genetic information. The percentage of cases in which the true diagnosis was placed at a given rank is shown on the Y axis. The X axis shows the ranks or rank groups. LIRICAL placed a total of 43.7% of cases in the top 3 ranks, and Phenomizer placed a total of 35.3% of cases in the top 3 ranks.

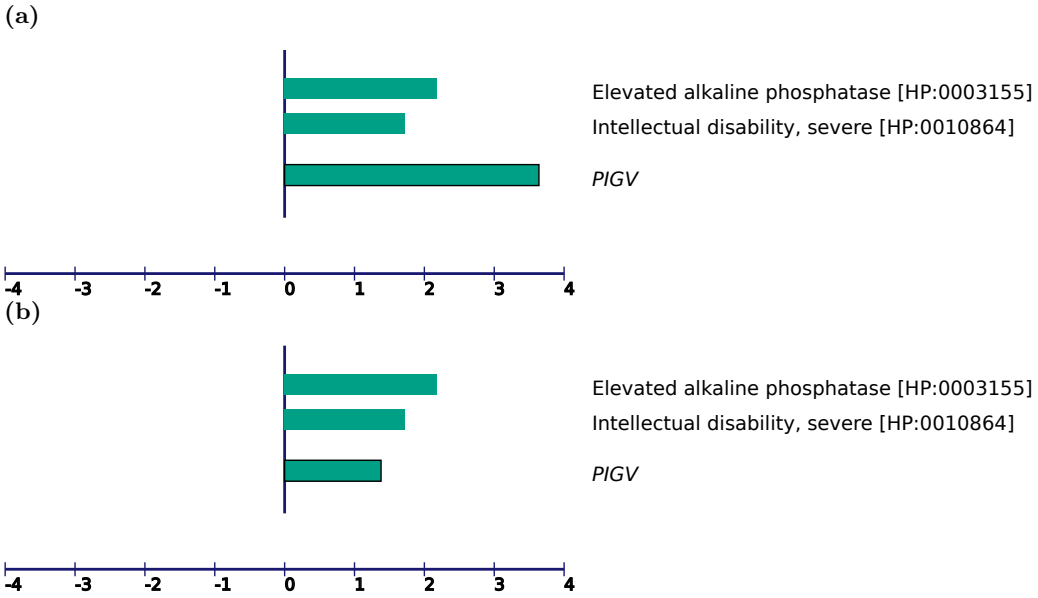

Figure S5. Ranking of an autosomal recessive disease with one pathogenic allele. Current exome and genome technologies can miss variants in highly GC-rich exons or can fail to detect structural variants. This may lead to only one of the expected two pathogenic alleles being identified for an autosomal recessive candidate disease. In this example, we show a simulated case of Hyperphosphatasia with mental retardation syndrome 1 (OMIM:239300) with two typical features. LIRICAL does not apply a hard filter to such cases but instead employs a flexible genotype likelihood ratio score. (a) Simulation with two pathogenic alleles; (b) Simulation in which one of the two alleles was removed. The LR for PIGV is lower but still contributory and the correct diagnosis remained in rank #1. The variants are chr1:27121140C>G (NM_001202554.1:c.615C>G, NP_001189483.1:p.(Asn205Lys)) and chr1:27121379A>G (NM_001202554.1:c.854A>G, NP_001189483.1:p.(Tyr285Cys)). Chromosomal coordinates are according to hg19.

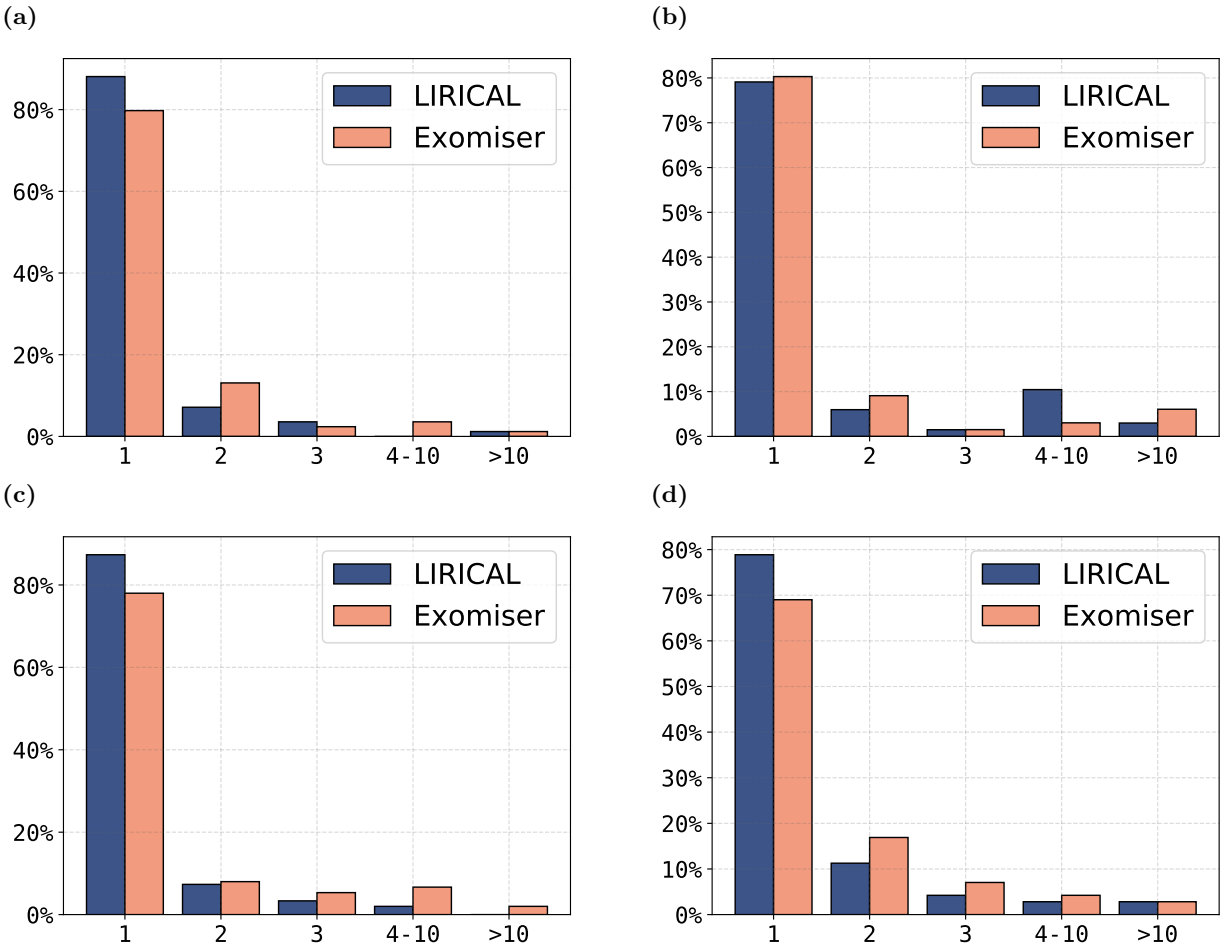

Figure S6. Performance of LIRICAL and Exomiser according to mode of inheritance and ClinVar status. The evaluation shown in Figure 2 of the main manuscript was repeated for subsets of the data. **(a)** Autosomal dominant diseases with disease-associated variant listed as pathogenic in ClinVar ($n = 84$); **(b)** Autosomal dominant diseases without variant listed as pathogenic in ClinVar ($n = 67$); **(c)** Autosomal recessive diseases with at least one disease-associated variant listed as pathogenic in ClinVar ($n = 150$); **(d)** Autosomal recessive diseases without variant listed as pathogenic in ClinVar ($n = 71$).

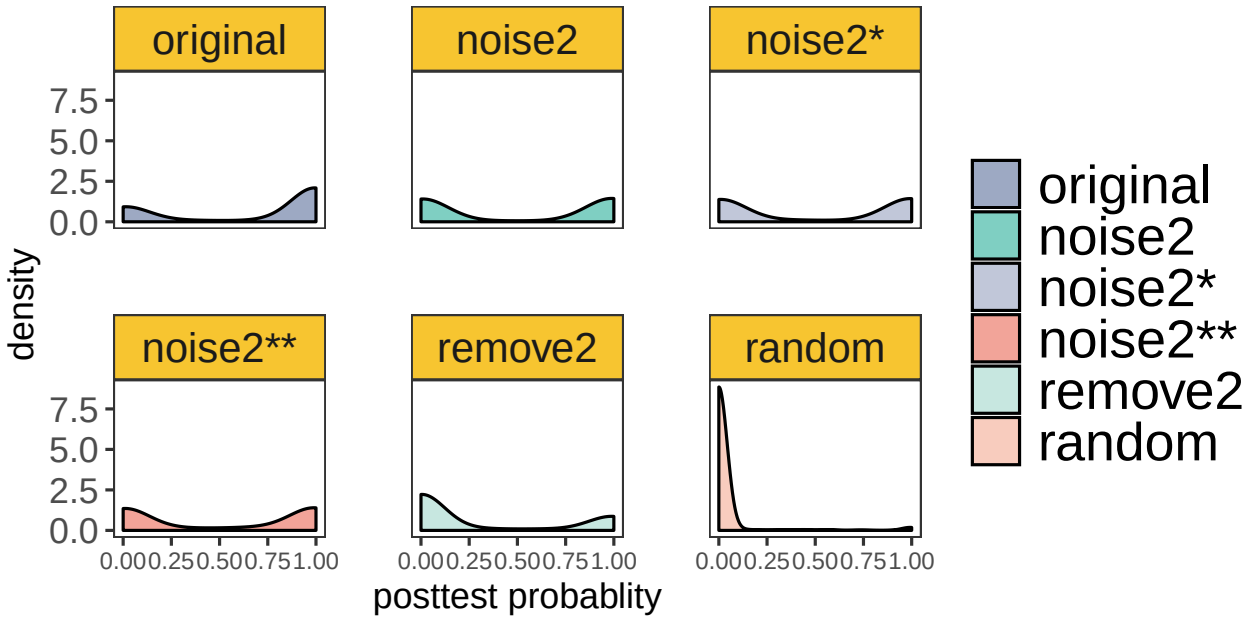

Figure S7. LIRICAL's posttest probability estimates. The post-test probability of the correct diagnosis was calculated for each of the 384 phenopacket case reports (Original). The mean post-test probability (pp) of the original data was 67.4%. Five procedures were applied to add noise to this data (Supplemental Table S3). Results for the original data are shown as `original`. `noise2`: two random HPO terms were added (mean pp: 50.8%); `noise2*`: two random HPO terms were added and original terms were replaced by parent terms (mean pp: 50.3%); `noise2**`: two random HPO terms were added and original terms were replaced by grandparent terms (mean pp:(mean pp: 50.3%); `remove2`: All pathogenic alleles were removed (mean pp: 29.4%); `random`: All HPO terms were replaced by random terms (mean pp: 2.9%).

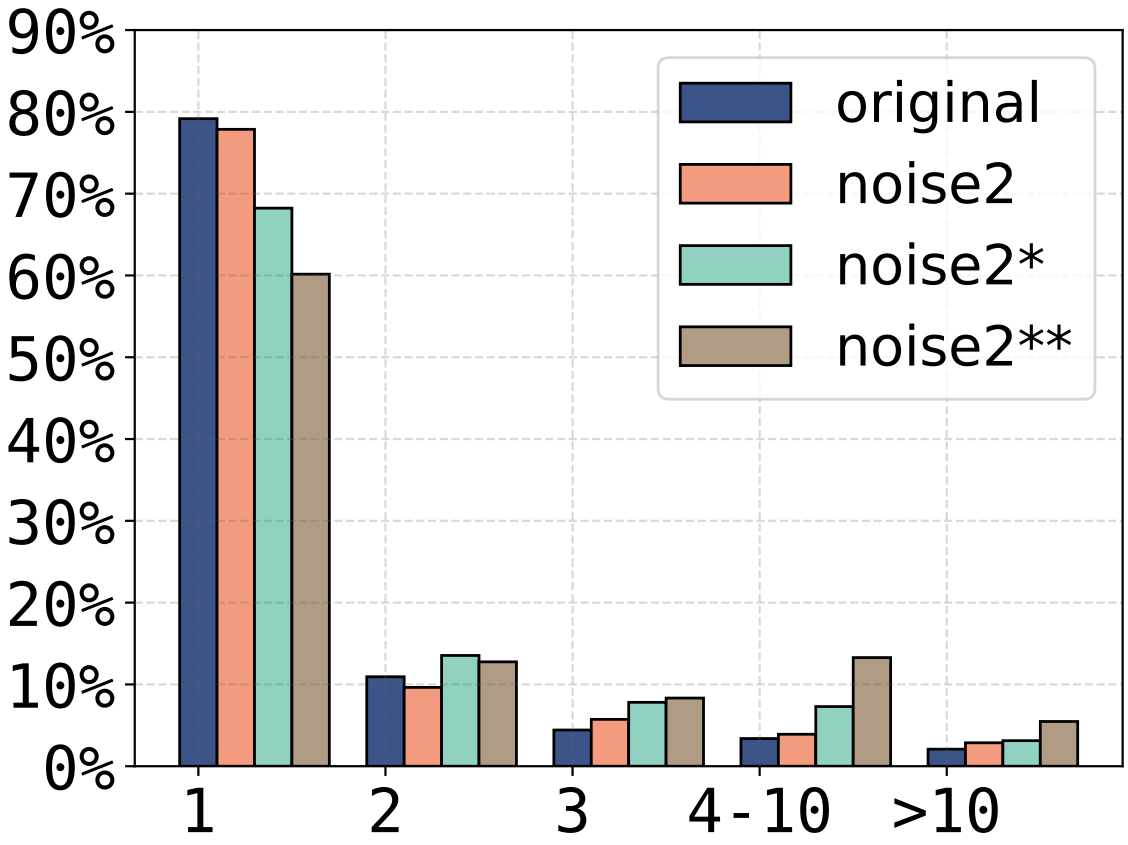

Figure S8. LIRICAL disease ranks. The ability of LIRICAL to predict the correct disease was assessed with 384 case reports (Table S2). This is the same simulation as presented in Fig. 2 of the main manuscript, but the rank is recorded for diseases instead of for disease genes. This is a harder prediction task because many genes are associated with multiple Mendelian diseases. Four tests were performed: `original`: unaltered data from the case reports. `noise2`: Two random ("noise") HPO terms are added to each case; `noise2*`: Original terms are replaced by a parent term and two noise terms are added; `noise2**`: Original terms are replaced by a grandparent term and two noise terms are added. The X axis shows the rank assigned by LIRICAL to the correct disease gene. The Y axis shows the percentage of cases in which the given rank was achieved.

(a)

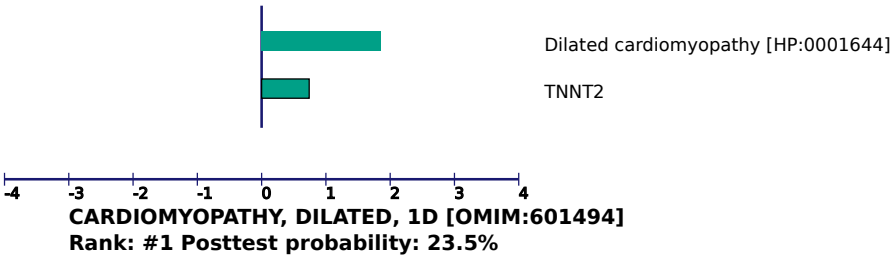

(b)

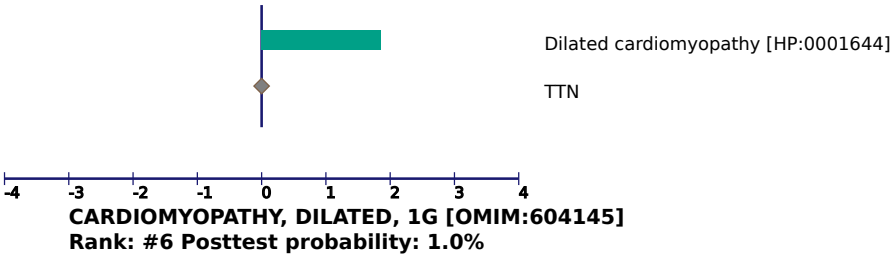

(c)

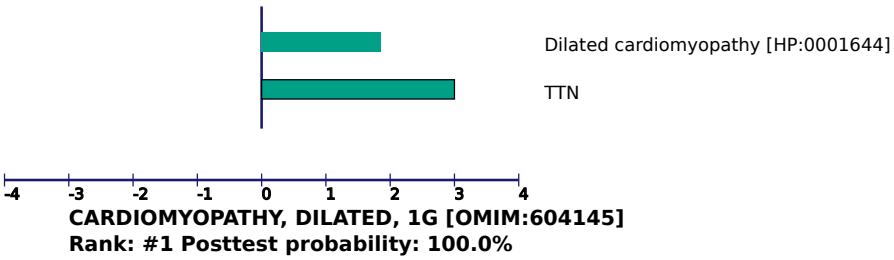

Figure S9. LIRICAL's treatment of ClinVar pathogenic variants. In this example, we simulate a patient with a rare (0.02% maximum population frequency) variant in *TTN*, NM_001267550.2(TTN):c.18295C>T [2], who is noted to have `Dilated cardiomyopathy` (HP:0001644). The variant is listed as having Uncertain significance in ClinVar (VCV000263438.2). **(a)** The candidate placed in rank 1 is a false positive, Dilated cardiomyopathy 1D (OMIM:601494) related to a variant in the *TNNT2* gene (NM_000364.3: c.683T>C, p.(Ile228Thr) that was present in the control VCF file. This variant is listed in ClinVar as having uncertain clinical significance (VCV000181604.2). **(b)** The correct candidate is placed at rank 6, Dilated cardiomyopathy 1G (OMIM:604145). The *TTN* mutation is scored with a likelihood ratio of just 2.70 in favor of OMIM:604145 because of the high background frequency of variants in this gene ($\lambda^{\mathcal{B}} = 9.4564$), despite the near maximal raw pathogenicity score of Exomiser (0.997). **(c)** In a separate simulation, the *TTN* variant NM_001267550.2:c.2926T>C (p.Trp976Arg) was spiked into the same control VCF file. This variant is listed in ClinVar as likely pathogenic (VCV000012651.3), and for this reason is (heuristically) assigned a likelihood ratio of 1000 by LIRICAL. The candidate is now correctly ranked in first place.

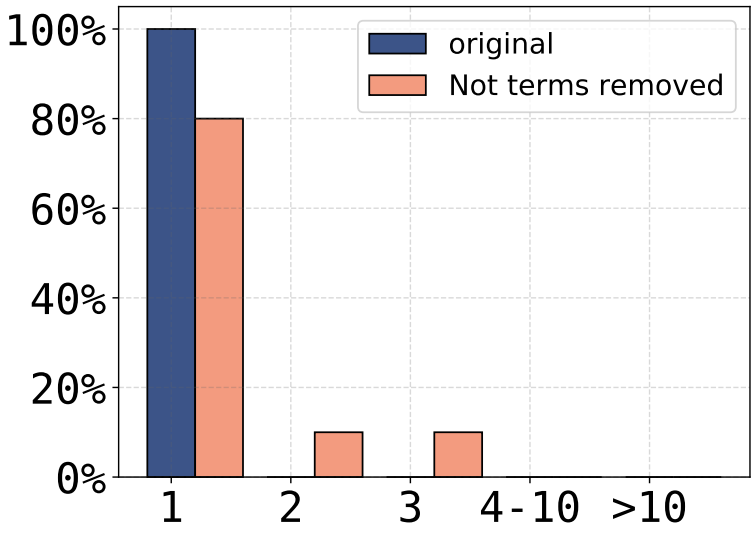

Figure S10. Negated annotations. LIRICAL was run with ten cases with a negated ("not") annotation deemed important for the differential diagnosis. For instance, Loeys-Dietz syndrome 4 is annotated not to have `Ectopia lentis`. Although the overall performance was good even without the negated annotations, in two of the ten cases, including the negated annotation boosted the rank of the correct candidate disease from 2 or 3 to 1. The X axis shows the rank assigned by LIRICAL to the correct disease gene. The Y axis shows the percentage of cases in which the given rank was achieved.

(a)

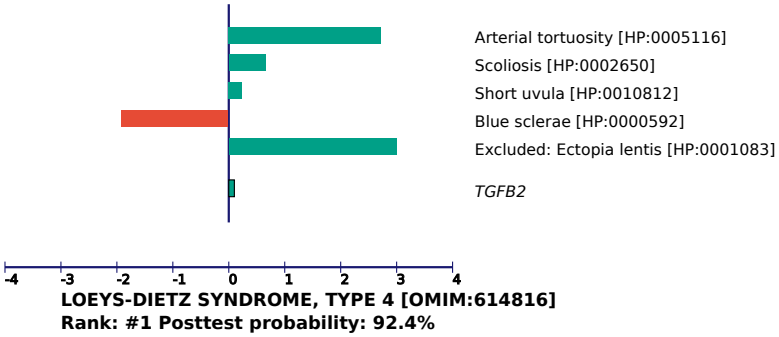

(b)

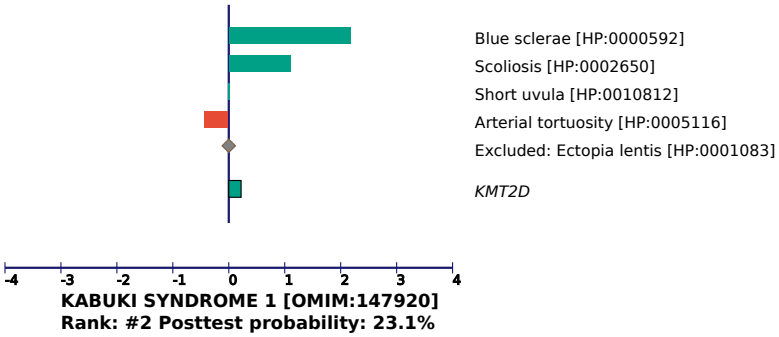

(c)

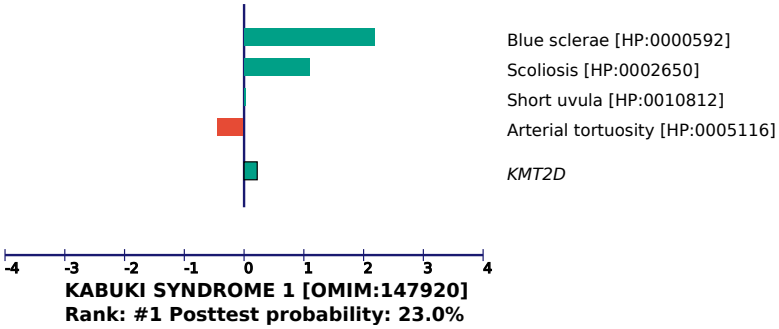

(d)

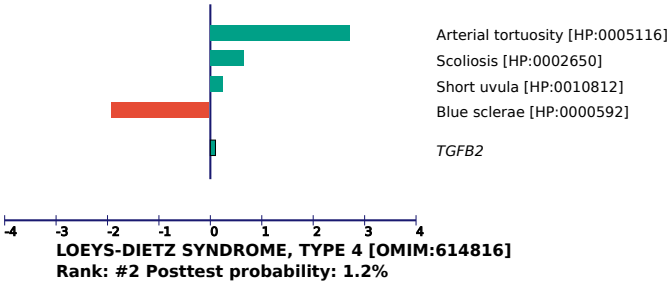

Figure S11. Ranking of candidate diseases with and without excluded features. In this example, panels **(a)** and **(b)** were run using a negated query term, `Ectopia lentis`, that had been excluded by examination of a hypothetical proband. Ranks 1 and 2 are shown. The correct diagnosis, Loeys-Dietz syndrome 4, has a posttest probability of 92.4%. In panels **(c)** and **(d)**, the excluded term was omitted and the correct diagnosis was placed in rank 2.

(a)

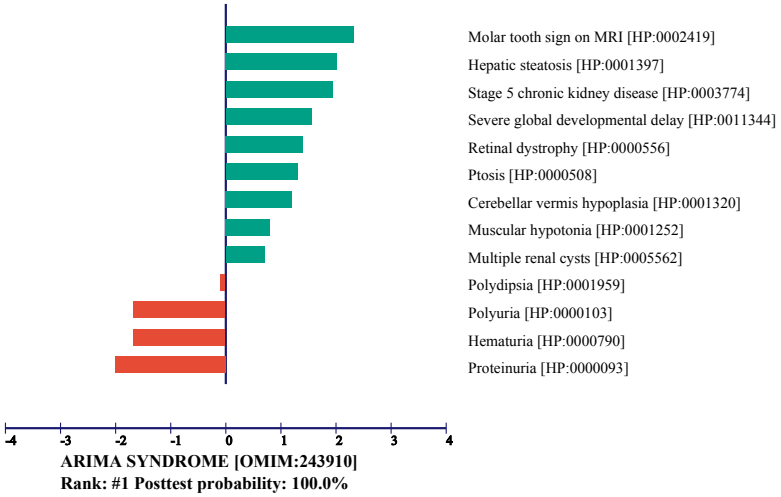

(b)

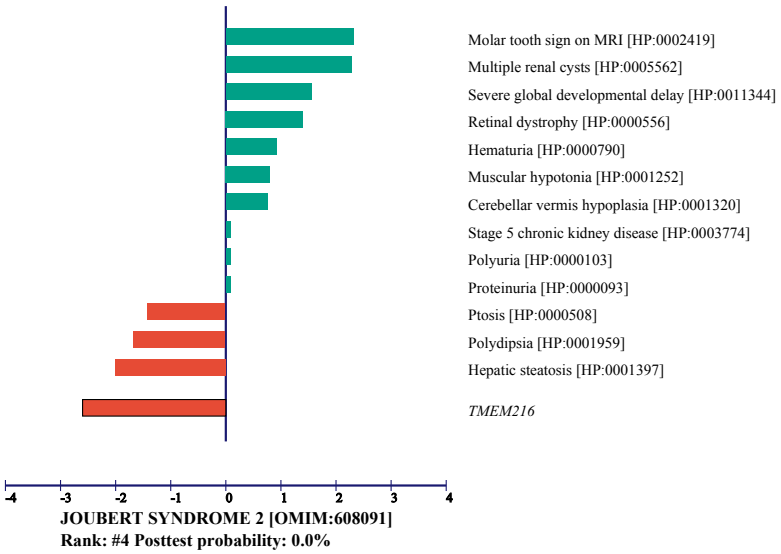

Figure S12. Assessment of diseases based only on clinical criteria. In this example, a case of Arima syndrome is simulated based on case 1 in a report on the clinicopathological features of the renal disease in Arima syndrome [3]. Arima syndrome shares many phenotypic features with Joubert syndrome. **(a)** In the simulated case using the control VCF file (without spiking in any pathogenic variant), Arima syndrome was correctly ranked in first place. **(b)** A type of Joubert syndrome was ranked in fourth place. No pathogenic alleles were identified in the causative gene *TMEM216*, which reduced the likelihood ratio (red bar corresponding to *TMEM216*).

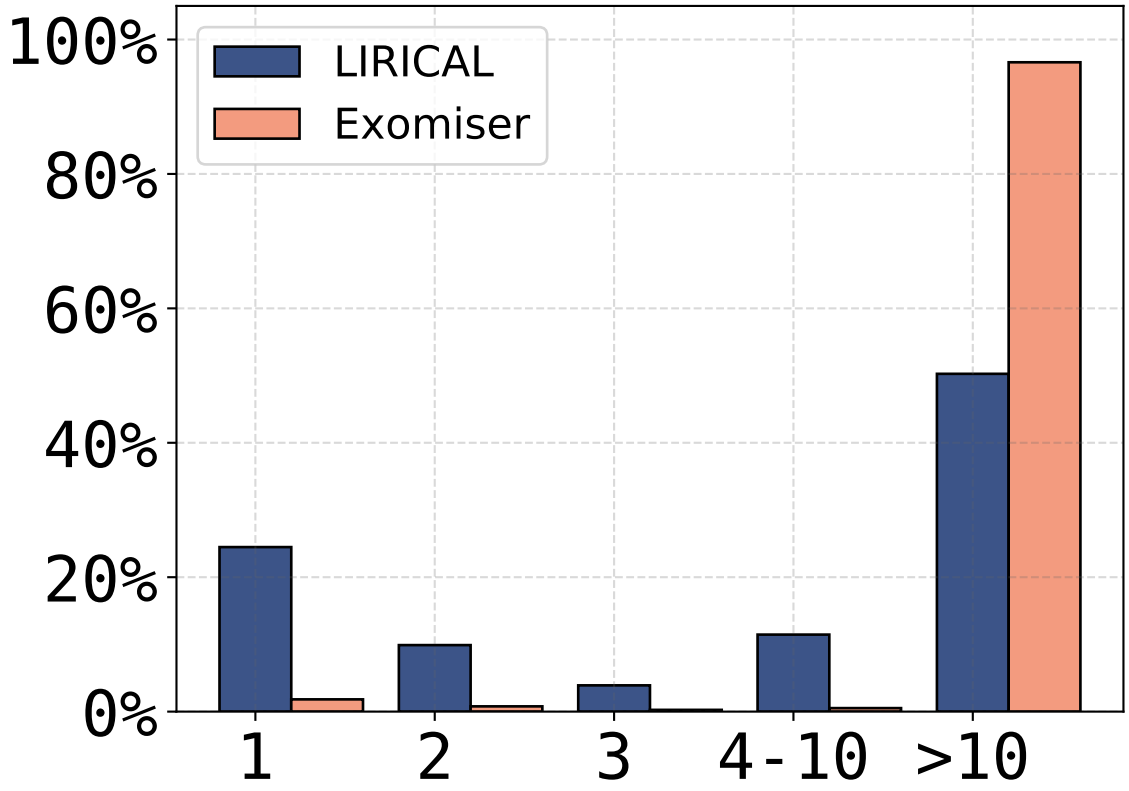

Figure S13. Rankings with all pathogenic alleles removed. Performance of LIRICAL (blue) and Exomiser (orange) on 384 case reports from which all pathogenic alleles have been removed from the VCF file. LIRICAL placed the correct candidate in the first ten ranks in 49.7% of cases, while Exomiser placed 4 of 384 candidates in rank 1 and failed to rank any of the other candidates. The X axis shows the rank assigned by LIRICAL or Exomiser to the correct disease gene. The Y axis shows the percentage of cases in which the given rank was achieved.

Gene	Frequency	Associated disease
TTN (7273)	9.46	CARDIOMYOPATHY, FAMILIAL HYPERTROPHIC, 9 (OMIM:613765)
HLA-DRB1 (3123)	9.29	SARCOIDOSIS, SUSCEPTIBILITY TO, 1 (OMIM:181000)
KRT18 (3875)	7.25	CIRRHOSIS, FAMILIAL (OMIM:215600)
FLG (2312)	5.98	DERMATITIS, ATOPIC, 2 (OMIM:605803)
NEB (4703)	5.29	NEMALINE MYOPATHY 2 (OMIM:256030)
MUC5B (727897)	4.99	PULMONARY FIBROSIS, IDIOPATHIC (OMIM:178500)
HLA-DQB1 (3119)	4.47	CELIAC DISEASE, SUSCEPTIBILITY TO, 1 (OMIM:212750)
SYNE2 (23224)	3.94	EMERY-DREIFUSS MUSCULAR DYSTROPHY 5, AUTOSOMAL DOMINANT (OMIM:612999)
SYN2 (6854)	3.71	SCHIZOPHRENIA (OMIM:181500)
RP1L1 (94137)	3.53	OCCULT MACULAR DYSTROPHY (OMIM:613587)
DSPP (1834)	3.38	DEAFNESS, AUTOSOMAL DOMINANT 39, WITH DENTINOGENESIS IMPERFECTA 1 (OMIM:605594)
FSIP2 (401024)	3.14	SPERMATOGENIC FAILURE 34 (OMIM:618153)
SCARF2 (91179)	3.11	VAN DEN ENDE-GUPTA SYNDROME (OMIM:600920)
ARMC9 (80210)	3.04	JOUBERT SYNDROME 30 (OMIM:617622)
DNAH11 (8701)	3.00	CILIARY DYSKINESIA, PRIMARY, 7 (OMIM:611884)
KMT2C (58508)	2.96	KLEEFSTRA SYNDROME 2 (OMIM:617768)
HLA-DQA1 (3117)	2.96	CELIAC DISEASE, SUSCEPTIBILITY TO, 1 (OMIM:212750)
EYS (346007)	2.87	RETINITIS PIGMENTOSA 25 (OMIM:602772)
HPS4 (89781)	2.73	HERMANSKY-PUDLAK SYNDROME 4 (OMIM:614073)
ALMS1 (7840)	2.54	ALSTROM SYNDROME (OMIM:203800)
FAT2 (2196)	2.47	SPINOCEREBELLAR ATAXIA 45 (OMIM:617769)
PIEZO1 (9780)	2.41	LYMPHATIC MALFORMATION 6 (OMIM:616843)
DST (667)	2.41	EPIDERMOLYSIS BULLOSA SIMPLEX, AUTOSOMAL RECESSIVE 2 (OMIM:615425)
ACAN (176)	2.37	SPONDYLOEPIMETAPHYSEAL DYSPLASIA, AGGRECAN TYPE (OMIM:612813)
HNF1A (6927)	2.37	DIABETES MELLITUS, INSULIN-DEPENDENT, 20 (OMIM:612520)
TNXB (7148)	2.35	VESICOURETERAL REFLUX 8 (OMIM:615963)
TRIOBP (11078)	2.33	DEAFNESS, AUTOSOMAL RECESSIVE 28 (OMIM:609823)
ISCU (23479)	2.29	MYOPATHY WITH LACTIC ACIDOSIS, HEREDITARY (OMIM:255125)
SON (6651)	2.21	ZTTK SYNDROME (OMIM:617140)
ADGRV1 (84059)	2.19	USHER SYNDROME, TYPE IIC (OMIM:605472)
TREH (11181)	2.16	TREHALASE DEFICIENCY (OMIM:612119)
SERPINA1 (5265)	2.11	ALPHA-1-ANTITRYPSIN DEFICIENCY (OMIM:613490)
FRRS1L (23732)	2.02	EPILEPTIC ENCEPHALOPATHY, EARLY INFANTILE, 37 (OMIM:616981)
FRG1 (2483)	2.01	FACIOSCAPULOHUMERAL MUSCULAR DYSTROPHY 1 (OMIM:158900)
CTU2 (348180)	1.95	MICROCEPHALY, FACIAL DYSMORPHISM, RENAL AGENESIS, AND AMBIGUOUS GENITALIA SYNDROME (OMIM:618142)
KRT13 (3860)	1.79	WHITE SPONGE NEVUS 2 (OMIM:615785)
STXBP2 (6813)	1.79	HEMOPHAGOCYTIC LYMPHOHISTIOCYTOSIS, FAMILIAL, 5 (OMIM:613101)
GEMIN4 (50628)	1.75	NEURODEVELOPMENTAL DISORDER WITH MICROCEPHALY, CATARACTS, AND RENAL ABNORMALITIES (OMIM:617913)
DUOX2 (50506)	1.75	THYROID DYSHORMONOGENESIS 6 (OMIM:607200)
A2ML1 (144568)	1.75	OTITIS MEDIA, SUSCEPTIBILITY TO (OMIM:166760)
APOL1 (8542)	1.71	FOCAL SEGMENTAL GLOMERULOSCLEROSIS 4, SUSCEPTIBILITY TO (OMIM:612551)
MYO5B (4645)	1.71	DIARRHEA 2, WITH MICROVILLUS ATROPHY (OMIM:251850)
TMEM216 (51259)	1.70	JOUBERT SYNDROME 2 (OMIM:608091)
LTBP4 (8425)	1.69	CUTIS LAXA, AUTOSOMAL RECESSIVE, TYPE IC (OMIM:613177)
PCLO (27445)	1.64	PONTOCEREBELLAR HYPOPLASIA, TYPE 3 (OMIM:608027)
KIZ (55857)	1.64	RETINITIS PIGMENTOSA 69 (OMIM:615780)
VCAN (1462)	1.61	WAGNER VITREORETINOPATHY (OMIM:143200)
VPS13B (157680)	1.61	COHEN SYNDROME (OMIM:216550)
RAI1 (10743)	1.60	SMITH-MAGENIS SYNDROME (OMIM:182290)
VWA3B (200403)	1.60	SPINOCEREBELLAR ATAXIA, AUTOSOMAL RECESSIVE 22 (OMIM:616948)
DHFR (1719)	1.58	MEGALOBLASTIC ANEMIA DUE TO DIHYDROFOLATE REDUCTASE DEFICIENCY (OMIM:613839)

Table S1. The 50 Mendelian disease-associated genes with the highest sum of population frequencies of called pathogenic variants.

Table S2. Phenopackets analyzed in this work.

Disease	Gene	Proband	n. HPO terms	Publication
Neurodevelopmental Disorder With Or Without Anomalies Of The Brain, Eye, Or Heart	RERE	Subject 9	84	PMID:27087320
Hypotonia, Infantile, With Psychomotor Retardation And Characteristic Facies 3	TBCK	6-2	5	PMID:27040691
Ectodermal Dysplasia 1, Hypohidrotic, X-Linked	EDA	proband	9	PMID:18702659
Deafness, Autosomal Recessive 7	TMC1	935-IV:1	2	PMID:18616530
Osteogenesis Imperfecta, Type Xiv	TMEM38B	family2-patient2	9	PMID:26911354
Cutis Laxa, Autosomal Recessive, Type Iic	ATP6V1E1	Family 5 - IV:2	4	PMID:27023906
Codas syndrome	LONP1	Proband	13	PMID:28148925
Thrombocythemia 2	MPL	FT2:VI:3	1	PMID:19036112
Parkinson Disease 23, Autosomal Recessive, Early Onset	VPS13C	VPS13C case	11	PMID:28862745
Nemaline Myopathy 4	TPM2	1A	5	PMID:23378224
Noonan syndrome 3	KRAS	Patient 2	14	PMID:17056636
Spinocerebellar Ataxia, Autosomal Recessive 20	SNX14	IV-1	18	PMID:30473892
Cleidocranial Dysplasia	RUNX2	Family-A-II1	19	PMID:31548836
Epileptic Encephalopathy, Early Infantile, 28	WWOX	Patient 1	18	PMID:27495153
Congenital Disorder Of Glycosylation, Type Iip	TMEM199	F1-II2	11	PMID:26833330
Loeys-Dietz syndrome 1	TGFBR1	patient	18	PMID:30701076
Ataxia-Pancytopenia syndrome	SAMD9L	P5	2	PMID:29217778
Branchiooculofacial syndrome	TFAP2A	10-year-old girl	13	PMID:20461149
Lowe Oculocerebrorenal syndrome	OCRL	Patient 1	8	PMID:29300302
Spastic Paraplegia 76, Autosomal Recessive	CAPN1	Fam1Pat1	7	PMID:29379883
Neurodevelopmental Disorder With Or Without Anomalies Of The Brain, Eye, Or Heart	RERE	Subject 7	88	PMID:27087320
Cerebral Creatine Deficiency syndrome 1	SLC6A8	proband	7	PMID:30400883
Epileptic Encephalopathy, Early Infantile, 14	KCNT1	Patient-1	5	PMID:24029078
Cutis Laxa, Autosomal Recessive, Type Iid	ATP6V1A	PV:1	11	PMID:28065471
Spastic Paraplegia 76, Autosomal Recessive	CAPN1	index	4	PMID:28566166
Cohen syndrome	VPS13B	proposita	18	PMID:29149870
Combined Oxidative Phosphorylation Deficiency 30	TRMT10C	Subject 1	18	PMID:27132592
Cutis Laxa, Autosomal Recessive, Type Iic	ATP6V1E1	PII:1	13	PMID:28065471
Hypotonia, Infantile, With Psychomotor Retardation And Characteristic Facies 3	TBCK	3-1	15	PMID:27040691
Nijmegen Breakage syndrome	NBN	12-year-old girl	18	PMID:24044622
Microcephaly 6, Primary, Autosomal Recessive	CENPJ	IV-5	7	PMID:16900296
Spondylocostal Dysostosis 1, Autosomal Recessive	DLL3	II.6	6	PMID:15200511
Microcephaly 3, Primary, Autosomal Recessive	CDK5RAP2	patient	6	PMID:23726037
Aarskog-Scott syndrome	FGD1	II-1	10	PMID:23211637
Bardet-Biedl syndrome 4	BBS4	4-year-old female patient	10	PMID:25533820
Muscular Dystrophy, Limb-Girdle, Type 2z	POGLUT1	Patient II.1	13	PMID:27807076
Neurodevelopmental Disorder With Or Without Anomalies Of The Brain, Eye, Or Heart	RERE	Subject 7	38	PMID:29330883

Continued on next page

Table S2 – *Continued from previous page*

Disease	**Gene**	**Proband**	**n. HPO terms**	**Publication**
Mental Retardation, Autosomal Dominant 42	GNB1	proband	10	PMID:29174093
Ataxia-Pancytopenia syndrome	SAMD9L	UB085	12	PMID:29146883
Neurodevelopmental Disorder With Or Without Anomalies Of The Brain, Eye, Or Heart	RERE	Subject 8	37	PMID:29330883
Cornelia De Lange syndrome 1	NIPBL	Patient 1	14	PMID:25447906
Tietz syndrome	MITF	family 815	6	PMID:10851256
Neurodevelopmental Disorder With Or Without Anomalies Of The Brain, Eye, Or Heart	RERE	Subject 6	13	PMID:29330883
Papillon-Lefevre syndrome	CTSC	Case 1P1	6	PMID:23311634
Neurodevelopmental Disorder With Or Without Anomalies Of The Brain, Eye, Or Heart	RERE	Subject 3	35	PMID:29330883
Townes-Brocks syndrome	SALL1	VMFS	23	PMID:29110636
Retinitis Pigmentosa 18	PRPF3	020001-II:4	4	PMID:27886254
Ataxia-Pancytopenia syndrome	SAMD9L	UB081	7	PMID:29146883
Bernard-Soulier syndrome	GP1BA	Patient 3	10	PMID:26044173
Ehlers-Danlos syndrome, Classic Type	COL5A1	AN-002501	9	PMID:23587214
Neurodevelopmental Disorder With Or Without Anomalies Of The Brain, Eye, Or Heart	RERE	Subject 10	6	PMID:27087320
Retinitis Pigmentosa With Or Without Skeletal Anomalies	CWC27	II-4	11	PMID:28285769
Metabolic Encephalomyopathic Crises, Recurrent, With Rhabdomyolysis, Cardiac Arrhythmias, And Neurodegeneration	TANGO2	Subject 5	21	PMID:26805781
Neurodevelopmental Disorder With Or Without Anomalies Of The Brain, Eye, Or Heart	RERE	Subject 8	93	PMID:27087320
Hajdu-Cheney syndrome	NOTCH2	proband	12	PMID:23566664
Retinitis Pigmentosa 11	PRPF31	IV:3	5	PMID:30099644
Intellectual Developmental Disorder With Dysmorphic Facies And Ptosis	BRPF1	Individual 11/Family F	11	PMID:27939639
Treacher Collins syndrome 2	POLR1D	family 1:patient	4	PMID:24603435
Amyloidosis, Finnish Type	GSN	III:5	6	PMID:26915616
Legius syndrome	SPRED1	P62	2	PMID:28150585
Neuropathy, Hereditary Sensory And Autonomic, Type Iib	RETREG1	F2:IV:1	8	PMID:30643655
Spastic Paraplegia 76, Autosomal Recessive	CAPN1	Fam2Pat1	7	PMID:29379883
Myhre syndrome	SMAD4	patient	18	PMID:24715504
Thrombocytopenia 3	FYB1	IV:5	4	PMID:25516138
Homocystinuria Due To Cystathionine Beta-Synthase Deficiency	CBS	patient	4	PMID:8755636
Albinism, Oculocutaneous, Type Iii	TYRP1	patient 2	3	PMID:21739261
Rett syndrome, Congenital Variant	FOXG1	Patient 2	11	PMID:28851325
Emery-Dreifuss Muscular Dystrophy 3, Autosomal Recessive	LMNA	II3	12	PMID:23313286
Spastic Ataxia 8, Autosomal Recessive, With Hypomyelinating Leukodystrophy	NKX6-2	IV-6	4	PMID:28575651
Oliver-Mcfarlane syndrome	PNPLA6	18 year-old female	17	PMID:30097146
Metabolic Encephalomyopathic Crises, Recurrent, With Rhabdomyolysis, Cardiac Arrhythmias, And Neurodegeneration	TANGO2	F1:II.2	23	PMID:26805782

Continued on next page

Table S2 – *Continued from previous page*

Disease	**Gene**	**Proband**	**n. HPO terms**	**Publication**
Ehlers-Danlos syndrome, Classic-Like, 2	AEBP1	AN-006205	23	PMID:30759870
Gm1-Gangliosidosis, Type Iii	GLB1	KT	6	PMID:1907800
Hyperoxaluria, Primary, Type Ii	GRHPR	patient	11	PMID:28569194
Bethlem Myopathy 1	COL6A1	II.1	21	PMID:30808312
Immunoskeletal Dysplasia With Neurodevelopmental Abnormalities	EXTL3	Patient 2	8	PMID:28148688
Ehlers-Danlos syndrome, Musculocontractural Type 1	CHST14	3-year old boy	16	PMID:30249733
Stankiewicz-Isidor syndrome	PSMD12	Subject 2	30	PMID:28132691
Marfan syndrome	FBN1	B15	7	PMID:11175294
Nemaline Myopathy 3	ACTA1	Patient 5	10	PMID:30517146
Fanconi Anemia, Complementation Group C	FANCC	proband	7	PMID:22701786
Autoimmune Polyendocrine syndrome, Type I, With Or Without Reversiblemetaphyseal Dysplasia	AIRE	V-1	10	PMID:28540407
Noonan syndrome 6	NRAS	case 1	15	PMID:26467218
Mental Retardation, Autosomal Recessive 38	HERC2	Pedigree 1A,VIII:8	9	PMID:23243086
Marfan syndrome	FBN1	Patient 2	11	PMID:30101859
Retinitis Pigmentosa With Or Without Skeletal Anomalies	CWC27	3:II-1	2	PMID:28285769
Cockayne syndrome B	ERCC6	index	18	PMID:30113454
Neuropathy, Hereditary Sensory And Autonomic, Type Iia	WNK1	Patient	13	PMID:16636245
Hypotonia, Infantile, With Psychomotor Retardation And Characteristic Facies 3	TBCK	A-II-1	28	PMID:27040692
Elliptocytosis 2	SPTA1	proband	10	PMID:29484404
Spastic Paraplegia 76, Autosomal Recessive	CAPN1	II-4	5	PMID:29678961
Hypotonia, Infantile, With Psychomotor Retardation And Characteristic Facies 3	TBCK	B-IV-6	16	PMID:27040692
Homocystinuria Due To Cystathionine Beta-Synthase Deficiency	CBS	III:3	12	PMID:26667307
Ataxia-Pancytopenia syndrome	SAMD9L	UB049	7	PMID:29146883
Waardenburg syndrome, Type 3	PAX3	proposita	8	PMID:12949970
Immunoskeletal Dysplasia With Neurodevelopmental Abnormalities	EXTL3	D:IV-1	23	PMID:28132690
Osteogenesis Imperfecta, Type Xi	FKBP10	proband	9	PMID:29801479
Retinitis Pigmentosa 27	NRL	II:2	4	PMID:28106895
Cutis Laxa, Autosomal Recessive, Type Ia	FBLN5	4-year-old Burmese girl	12	PMID:24962763
Rubinstein-Taybi syndrome 2	EP300	11	26	PMID:29506490
Amelogenesis Imperfecta, Type Ij	ACP4	Family 1-IV:3	2	PMID:28513613
Osteogenesis Imperfecta, Type Viii	P3H1	proband	4	PMID:27864101
Cornelia De Lange syndrome 3	SMC3	patient 1	23	PMID:28781842
3-@methylglutaconic Aciduria With Deafness, Encephalopathy, And Leigh-Likesyndrome	SERAC1	proband	23	PMID:31251474
Neurodevelopmental Disorder With Or Without Anomalies Of The Brain, Eye, Or Heart	RERE	Subject 2	84	PMID:27087320
Geleophysic Dysplasia 1	ADAMTSL2	patient	16	PMID:27057656

Continued on next page

Table S2 – *Continued from previous page*

Disease	**Gene**	**Proband**	**n. HPO terms**	**Publication**
Parkinson Disease 23, Autosomal Recessive, Early Onset	VPS13C	Family B, II-1	5	PMID:26942284
Spastic Ataxia 8, Autosomal Recessive, With Hypomyelinating Leukodystrophy	NKX6-2	Patient 4 II-1	10	PMID:28969374
Myopathy, Distal, Tateyama Type	CAV3	I1	16	PMID:18930476
Ataxia-Pancytopenia syndrome	SAMD9L	III-1	10	PMID:28202457
Stankiewicz-Isidor syndrome	PSMD12	Subject 3	12	PMID:28132691
Arthrogryposis, Distal, Type 2a	MYH3	proband	13	PMID:28584669
Polymicrogyria With Seizures	RTTN	Patient 3	10	PMID:29883675
Cutis Laxa, Autosomal Recessive, Type Iid	ATP6V1A	PIV:1	19	PMID:28065471
Glycogen Storage Disease Vi	PYGL	2-year 5-month old child	14	PMID:28984260
Polyarteritis Nodosa, Childhood-Onset	ADA2	patient 1	13	PMID:28830446
Bardet-Biedl syndrome 1	BBS1	IV-5/family A	7	PMID:23559858
Arthrogryposis, Distal, With Impaired Proprioception And Touch	PIEZO2	Patient	12	PMID:27974811
Hypotonia, Infantile, With Psychomotor Retardation And Characteristic Facies 3	TBCK	2-1	12	PMID:27040691
Severe Combined Immunodeficiency, Autosomal Recessive, T Cell-Negative,b Cell-Negative, Nk Cell-Negative, Due To Adenosine Deaminase Deficiency	ADA	Patient	6	PMID:1680289
Hypotonia, Infantile, With Psychomotor Retardation And Characteristic Facies 3	TBCK	Patient 2	16	PMID:30103036
Spastic Ataxia 8, Autosomal Recessive, With Hypomyelinating Leukodystrophy	NKX6-2	Patient 36-16DG1123	5	PMID:28940097
Neurodevelopmental Disorder With Or Without Anomalies Of The Brain, Eye, Or Heart	RERE	Subject 5	31	PMID:29330883
Structural Heart Defects And Renal Anomalies syndrome	TMEM260	1-II-1	23	PMID:28318500
Cone-Rod Dystrophy 2	CRX	IV:5	4	PMID:30095615
Hypotonia, Infantile, With Psychomotor Retardation And Characteristic Facies 3	TBCK	B-IV-4	24	PMID:27040692
Smith-Lemli-Opitz syndrome	DHCR7	patient	13	PMID:28503313
Congenital Disorder Of Glycosylation, Type Il	ALG9	IV:5	16	PMID:26453364
Nephrotic syndrome, Type 1	NPHS1	patient 1	9	PMID:28392951
Neurodevelopmental Disorder With Or Without Anomalies Of The Brain, Eye, Or Heart	RERE	Subject 3	96	PMID:27087320
Acromesomelic Dysplasia, Maroteaux Type	NPR2	IV-2/family-A	10	PMID:25959430
Ayme-Gripp syndrome	MAF	patient CSA108.01	1	PMID:28482824
Spastic Paraplegia 76, Autosomal Recessive	CAPN1	SAL-399-073	7	PMID:27320912
Geleophysic Dysplasia 2	FBN1	Family 1, Patient 1	14	PMID:29191498
Robinow syndrome, Autosomal Recessive	ROR2	Patient 1	20	PMID:24932600
Parkinson Disease 23, Autosomal Recessive, Early Onset	VPS13C	Family C, II-1	4	PMID:26942284
Wiedemann-Steiner syndrome	KMT2A	P1	16	PMID:25186178

Continued on next page

Table S2 – *Continued from previous page*

Disease	**Gene**	**Proband**	**n. HPO terms**	**Publication**
Diarrhea 8, Secretory Sodium, Congenital	SLC9A3	Patient 9	9	PMID:26358773
Spastic Paraplegia 76, Autosomal Recessive	CAPN1	Index	7	PMID:28321562
Retinitis Pigmentosa With Or Without Skeletal Anomalies	CWC27	4:II-3	14	PMID:28285769
Spastic Paraplegia 7, Autosomal Recessive	SPG7	II-3	13	PMID:17646629
Hyaline Fibromatosis syndrome	ANTXR2	II-3	13	PMID:30050362
Cleidocranial Dysplasia	RUNX2	Family-B-II1	19	PMID:31548836
Heterotaxy, Visceral, 1, X-Linked	ZIC3	III-1	12	PMID:9354794
Autoimmune Lymphoproliferative syndrome	FASLG	patient	14	PMID:22857792
Immunoskeletal Dysplasia With Neurodevelopmental Abnormalities	EXTL3	E:II-1	20	PMID:28132690
Muenke syndrome	FGFR3	Proband 27	5	PMID:26740388
Congenital Disorder Of Glycosylation, Type Iip	TMEM199	Patient 1	7	PMID:29321044
Marfan syndrome	FBN1	Patient 1	4	PMID:30101859
Mental Retardation, Autosomal Dominant 7	DYRK1A	Patient 2	19	PMID:26922654
Immunoskeletal Dysplasia With Neurodevelopmental Abnormalities	EXTL3	Patient 1	50	PMID:28331220
Van Den Ende-Gupta syndrome	SCARF2	proband	17	PMID:29378527
Bartter syndrome, Type 4a	BSND	family-A-III3	9	PMID:18776122
Loeys-Dietz syndrome 3	SMAD3	54-year old woman	2	PMID:28286188
Holoprosencephaly 5	ZIC2	proband	3	PMID:30855487
Epidermolysis Bullosa, Junctional, Herlitz Type	LAMC2	patient	5	PMID:24533970
Neurodevelopmental Disorder With Or Without Anomalies Of The Brain, Eye, Or Heart	RERE	Subject 6	78	PMID:27087320
Apert syndrome	FGFR2	Patient 1	14	PMID:23546041
Stankiewicz-Isidor syndrome	PSMD12	Subject 4	21	PMID:28132691
Myasthenic syndrome, Congenital, 8	AGRN	Patient 3/Kinship 2	15	PMID:24951643
Donohue syndrome	INSR	ISR1	14	PMID:24498630
Cornelia De Lange syndrome 1	NIPBL	Patient 2	10	PMID:25447906
Microcephaly 5, Primary, Autosomal Recessive	ASPM	patient	10	PMID:29644084
Hypothyroidism, Thyroidal Or Athyroidal, With Spiky Hair And Cleftpalate	FOXE1	patient	7	PMID:24219130
Fanconi Anemia, Complementation Group I	FANCI	NCI-309-1	9	PMID:26590883
Hypotonia, Infantile, With Psychomotor Retardation And Characteristic Facies 3	TBCK	1-1	20	PMID:27040691
Camurati-Engelmann Disease	TGFB1	patient	13	PMID:30034812
Bernard-Soulier syndrome	GP1BA	73 year old male	5	PMID:9233564
Immunoskeletal Dysplasia With Neurodevelopmental Abnormalities	EXTL3	AII-1	14	PMID:28132690
Galloway-Mowat syndrome 4	TP53RK	II-1	10	PMID:30053862
Leukocyte Adhesion Deficiency, Type I	ITGB2	P1	4	PMID:26497373
Spastic Paraplegia 76, Autosomal Recessive	CAPN1	Family B-IV:1	7	PMID:27153400
Ataxia-Pancytopenia syndrome	SAMD9L	II-4	13	PMID:28202457
Hypotonia, Infantile, With Psychomotor Retardation And Characteristic Facies 3	TBCK	8-1	14	PMID:27040691
Trichothiodystrophy 3, Photosensitive	GTF2H5	male infant	27	PMID:30359777

Continued on next page

Table S2 – *Continued from previous page*

Disease	**Gene**	**Proband**	**n. HPO terms**	**Publication**
Deafness, Autosomal Recessive 15	GIPC3	Ahv-14:23	1	PMID:29605370
Galactosemia	GALT	FKT118	7	PMID:25681079
Vici syndrome	EPG5	18-month son	15	PMID:29983806
Immunoskeletal Dysplasia With Neurodevelopmental Abnormalities	EXTL3	B:II-2	28	PMID:28132690
Sick Sinus syndrome 2, Autosomal Dominant	HCN4	family A/II:1	3	PMID:25145518
Charcot-Marie-Tooth Disease, Demyelinating, Type 1c	LITAF	Proband	14	PMID:19541485
Chudley-Mccullough syndrome	GPSM2	case 1	13	PMID:27180139
Schinzel-Giedion Midface Retraction syndrome	SETBP1	proposita	26	PMID:29333303
Orofaciodigital syndrome V	DDX59	Patient 1	11	PMID:29127725
Ventricular Tachycardia, Catecholaminergic Polymorphic, 1, With Orwithout Atrial Dysfunction And/or Dilated Cardiomyopathy	RYR2	proband	6	PMID:30296944
Long Qt syndrome 15	CALM2	Case 1	4	PMID:27374306
Cleidocranial Dysplasia	RUNX2	Family-D-II1	19	PMID:31548836
Renal Cysts And Diabetes syndrome	HNF1B	patient	6	PMID:29491316
Ataxia-Pancytopenia syndrome	SAMD9L	II-4	6	PMID:27259050
Acromicric Dysplasia	FBN1	patient	17	PMID:27834076
Neurodevelopmental Disorder With Or Without Anomalies Of The Brain, Eye, Or Heart	RERE	Subject 2	22	PMID:29330883
Hypotonia, Infantile, With Psychomotor Retardation And Characteristic Facies 3	TBCK	II-4	16	PMID:27275012
Intellectual Developmental Disorder With Dysmorphic Facies, Seizures, And Distal Limb Anomalies	OTUD6B	proband	14	PMID:30364145
Spastic Ataxia 8, Autosomal Recessive, With Hypomyelinating Leukodystrophy	NKX6-2	Patient 3 II-3	9	PMID:28969374
Fibrodysplasia Ossificans Progressiva	ACVR1	patient	10	PMID:29482508
Neurodegeneration With Brain Iron Accumulation 1	PANK2	Family I patient I	7	PMID:28821231
Al Kaissi syndrome	CDK10	F1-II:1	20	PMID:28886341
Neurodevelopmental Disorder With Or Without Anomalies Of The Brain, Eye, Or Heart	RERE	Subject 5	92	PMID:27087320
Hypotrichosis, Congenital, With Juvenile Macular Dystrophy	CDH3	Patient	14	PMID:28061825
Epileptic Encephalopathy, Early Infantile, 4	STXBP1	P1	6	PMID:29896790
Myopathy, Centronuclear, 1	DNM2	Patient 1	12	PMID:24465259
Hypotonia, Infantile, With Psychomotor Retardation And Characteristic Facies 3	TBCK	C-II-1	26	PMID:27040692
Apert syndrome	FGFR2	Patient 2	16	PMID:23546041
Kufor-Rakeb syndrome	ATP13A2	Case 1	12	PMID:30746398
Hypotonia, Infantile, With Psychomotor Retardation And Characteristic Facies 3	TBCK	4-2	4	PMID:27040691
Ichthyosis, Congenital, Autosomal Recessive 11	ST14	patient	7	PMID:18445049
Alzheimer Disease 4	PSEN2	proband	3	PMID:30104866
Immunoskeletal Dysplasia With Neurodevelopmental Abnormalities	EXTL3	Patient 3	28	PMID:28148688
Congenital Disorder Of Glycosylation, Type Iip	TMEM199	F2-II2	17	PMID:26833330

Continued on next page

Table S2 – *Continued from previous page*

Disease	**Gene**	**Proband**	**n. HPO terms**	**Publication**
Hypotonia, Infantile, With Psychomotor Retardation And Characteristic Facies 3	TBCK	4-1	10	PMID:27040691
Tuberous Sclerosis 2	TSC2	III-1	4	PMID:8825048
Osteogenesis Imperfecta, Type Ix	PPIB	second fetus	5	PMID:28242392
Spastic Paraplegia 76, Autosomal Recessive	CAPN1	Tun66275	3	PMID:27320912
Chitayat syndrome	ERF	proband	17	PMID:30569521
Charge syndrome	CHD7	Patient A III-2	14	PMID:17661815
Cholestasis, Progressive Familial Intrahepatic, 4	TJP2	proband	17	PMID:30658709
Congenital Disorder Of Glycosylation, Type Iip	TMEM199	Patient 3	6	PMID:29321044
Osteogenesis Imperfecta, Type Xii	SP7	II:5	16	PMID:29382611
Ectodermal Dysplasia 9, Hair/nail Type	HOXC13	IV-1	7	PMID:28403827
Diamond-Blackfan Anemia 1	RPS19	patient	5	PMID:27732904
Spinal Muscular Atrophy With Progressive Myoclonic Epilepsy	ASAH1	patient	13	PMID:31213928
Cutis Laxa, Autosomal Recessive, Type Iib	PYCR1	Patient 4	16	PMID:21487760
Intellectual Developmental Disorder With Dysmorphic Facies And Behavioral Abnormalities	FBXO11	Individual 1	26	PMID:30057029
Nemaline Myopathy 1	TPM3	II.2	20	PMID:24239060
Skraban-Deardorff syndrome	WDR26	Individual 1, PPMD01P, GEA055P	53	PMID:28686853
Stankiewicz-Isidor syndrome	PSMD12	Subject 1	34	PMID:28132691
Myasthenic syndrome, Congenital, 9, Associated With Acetylcholinereceptor Deficiency	MUSK	patient	17	PMID:23326516
Neurodevelopmental Disorder With Progressive Microcephaly, Spasticity, And Brain Anomalies	PLAA	Family A-IV:6	22	PMID:28413018
Peutz-Jeghers syndrome	STK11	20-year-old woman	3	PMID:15200509
Structural Heart Defects And Renal Anomalies syndrome	TMEM260	2-II-4	19	PMID:28318500
Spherocytosis, Type 4	SLC4A1	c.1432-2A¿T	3	PMID:23255290
Spastic Ataxia 8, Autosomal Recessive, With Hypomyelinating Leukodystrophy	NKX6-2	III-1	19	PMID:28575651
Multiple Endocrine Neoplasia, Type I	MEN1	III-3	15	PMID:26239674
Hyper-Ige Recurrent Infection syndrome, Autosomal Dominant	STAT3	12 year old girl	12	PMID:20149460
Stickler syndrome, Type Ii	COL11A1	proband	9	PMID:28971234
Congenital Disorder Of Glycosylation, Type Iip	TMEM199	Patient 2	7	PMID:29321044
Spastic Paraplegia 45, Autosomal Recessive	NT5C2	II.3	13	PMID:28327087
Werner syndrome	WRN	48-year-old male	18	PMID:30891318
Alagille syndrome 1	JAG1	Proband	18	PMID:30046498
Corneal Dystrophy, Fuchs Endothelial, 4	SLC4A11	Patient 1	2	PMID:25007886
Parkinson Disease 23, Autosomal Recessive, Early Onset	VPS13C	Family A, V-2	18	PMID:26942284
Congenital Disorder Of Glycosylation, Type Iip	TMEM199	F3-II1	12	PMID:26833330
Epidermolysis Bullosa, Junctional, Herlitz Type	LAMA3	Proband	2	PMID:20881434
Mucolipidosis Ii Alpha/beta	GNPTAB	proband	14	PMID:30208878
Combined Oxidative Phosphorylation Deficiency 30	TRMT10C	Subject 2	15	PMID:27132592

Continued on next page

Table S2 – *Continued from previous page*

Disease	**Gene**	**Proband**	**n. HPO terms**	**Publication**
Stickler syndrome, Type I	COL2A1	proband	19	PMID:28841907
Myotonia Congenita, Autosomal Dominant	CLCN1	man	7	PMID:30243293
Spondyloepimetaphyseal Dysplasia With Joint Laxity, Type 1, With Orwithout Fractures	B3GALT6	P7/F6	29	PMID:23664117
Hypotonia, Infantile, With Psychomotor Retardation And Characteristic Facies 3	TBCK	6-1	13	PMID:27040691
Tuberous Sclerosis 1	TSC1	II:3/Family 2	7	PMID:18830229
Weill-Marchesani syndrome 1	ADAMTS10	18-year-old woman	9	PMID:25469541
Megalocornea	CHRDL1	III-1	4	PMID:24073597
Hyperuricemic Nephropathy, Familial Juvenile, 1	UMOD	proband	6	PMID:15673476
Cutis Laxa, Autosomal Recessive, Type Iid	ATP6V1A	PIII:1	14	PMID:28065471
Spastic Ataxia 8, Autosomal Recessive, With Hypomyelinating Leukodystrophy	NKX6-2	F6,II-2	24	PMID:29388673
Tuberous Sclerosis 1	TSC1	patient 6	7	PMID:29196670
Retinitis Pigmentosa 78	ARHGEF18	Individual 1	8	PMID:28132693
Amelogenesis Imperfecta, Type Ia	LAMB3	proband	2	PMID:27220909
Bardet-Biedl syndrome 5	BBS5	II:2	6	PMID:30850397
Bleeding Disorder, Platelet-Type, 17	GFI1B	II:6	5	PMID:30655368
Nemaline Myopathy 7	CFL2	Patient 1	12	PMID:22560515
Neurodevelopmental Disorder With Progressive Microcephaly, Spasticity, And Brain Anomalies	PLAA	A-VI3	17	PMID:28007986
Bardet-Biedl syndrome 2	BBS2	II:2	9	PMID:26078953
Neurofibromatosis, Type I	NF1	0548	8	PMID:9101303
Gapo syndrome	ANTXR1	14 year old brother	11	PMID:27587992
Charcot-Marie-Tooth Disease, Axonal, Type 2a2	MFN2	patient	11	PMID:26956144
Platelet Disorder, Familial, With Associated Myeloid Malignancy	RUNX1	Pedigree I, V:2	3	PMID:28181366
Trichohepatoenteric syndrome 1	TTC37	index	17	PMID:28292286
Hypotonia, Infantile, With Psychomotor Retardation And Characteristic Facies 3	TBCK	Patient 1	30	PMID:30103036
Glutaric Acidemia I	GCDH	Patient 5	5	PMID:27672653
Choreoacanthocytosis	VPS13A	Patient-2	9	PMID:28446873
Ataxia-Pancytopenia syndrome	SAMD9L	P7	2	PMID:29217778
Albinism, Oculocutaneous, Type Ii	OCA2	B	4	PMID:29050284
Cockayne syndrome A	ERCC8	Patient A	7	PMID:30200888
Pseudoachondroplasia	COMP	patient	17	PMID:23562786
Galactosialidosis	CTSA	BAB3767	13	PMID:24769197
Neurodevelopmental Disorder With Progressive Microcephaly, Spasticity, And Brain Anomalies	PLAA	Family D-Case VIII-1	14	PMID:28413018
Cardiomyopathy, Dilated, 1g	TTN	JK109	4	PMID:11846417
Joubert syndrome 30	ARMC9	UW132-3	5	PMID:28625504
Dyskeratosis Congenita, Autosomal Dominant 3	TINF2	proband	12	PMID:29742735
Temtamy Preaxial Brachydactyly syndrome	CHSY1	IV-1	16	PMID:24269551
Krabbe Disease	GALC	child	6	PMID:26567009
Neurodevelopmental Disorder With Or Without Anomalies Of The Brain, Eye, Or Heart	RERE	Subject 4	16	PMID:29330883
Spastic Paraplegia 76, Autosomal Recessive	CAPN1	SAL-584-005	4	PMID:27320912

Continued on next page

Table S2 – *Continued from previous page*

Disease	**Gene**	**Proband**	**n. HPO terms**	**Publication**
Ataxia, Early-Onset, With Oculomotor Apraxia And Hypoalbuminemia	APTX	V-3	4	PMID:28652255
Retinitis Pigmentosa 78	ARHGEF18	Individual 2	8	PMID:28132693
Hypochondroplasia	FGFR3	VI-5	9	PMID:30681580
Hypotonia, Infantile, With Psychomotor Retardation And Characteristic Facies 3	TBCK	5-1	18	PMID:27040691
Immunoskeletal Dysplasia With Neurodevelopmental Abnormalities	EXTL3	BII-1	26	PMID:28132690
Spastic Paraplegia 76, Autosomal Recessive	CAPN1	Family A-V:2	8	PMID:27153400
Neurodevelopmental Disorder With Or Without Anomalies Of The Brain, Eye, Or Heart	RERE	Subject 1	88	PMID:27087320
Larsen syndrome	FLNB	patient	12	PMID:18322662
Muckle-Wells syndrome	NLRP3	proband	9	PMID:27435956
Leukocyte Adhesion Deficiency, Type Iii	FERMT3	index	4	PMID:31068971
Cardiofaciocutaneous syndrome 1	BRAF	CFC16	16	PMID:16474404
Ataxia-Pancytopenia syndrome	SAMD9L	UB612	3	PMID:29146883
Immunoskeletal Dysplasia With Neurodevelopmental Abnormalities	EXTL3	Patient 1	10	PMID:28148688
Metabolic Encephalomyopathic Crises, Recurrent, With Rhabdomyolysis, Cardiac Arrhythmias, And Neurodegeneration	TANGO2	Subject 6	17	PMID:26805781
Boucher-Neuhauser syndrome	PNPLA6	II.2	8	PMID:29749493
Nail-Patella syndrome	LMX1B	index	6	PMID:30881852
Neurodegeneration With Brain Iron Accumulation 2b	PLA2G6	family II patient II	8	PMID:28821231
Osteogenesis Imperfecta, Type Xv	WNT1	proband	11	PMID:30012084
Spastic Paraplegia 10, Autosomal Dominant	KIF5A	proband	12	PMID:30057544
Palmoplantar Keratoderma, Epidermolytic	KRT9	III:4	3	PMID:18477167
Cerebral Dysgenesis, Neuropathy, Ichthyosis, And Palmoplantar Keratodermasyndrome	SNAP29	The patient	19	PMID:29051910
Metabolic Encephalomyopathic Crises, Recurrent, With Rhabdomyolysis, Cardiac Arrhythmias, And Neurodegeneration	TANGO2	Suject 1	20	PMID:26805781
Spastic Ataxia 8, Autosomal Recessive, With Hypomyelinating Leukodystrophy	NKX6-2	Patient 1 II-1	13	PMID:28969374
Hyperekplexia, Hereditary 1	GLRA1	proband	5	PMID:24969041
Rett syndrome, Congenital Variant	FOXG1	Patient 4	9	PMID:28851325
Loeys-Dietz syndrome 4	TGFB2	proposita	15	PMID:25163805
Smith-Magenis syndrome	RAI1	SMS324	25	PMID:20932317
Metabolic Encephalomyopathic Crises, Recurrent, With Rhabdomyolysis, Cardiac Arrhythmias, And Neurodegeneration	TANGO2	Subject 4	16	PMID:26805781
Parkinson Disease 15, Autosomal Recessive Early-Onset	FBXO7	ANK-07	7	PMID:25085748
Alpha-Thalassemia/mental Retardation syndrome, X-Linked	ATRX	Proband	9	PMID:28371217
Rett syndrome, Congenital Variant	FOXG1	Patient 1	12	PMID:28851325
Smith-Kingsmore syndrome	MTOR	index	9	PMID:27753196
Trichorhinophalangeal syndrome, Type I	TRPS1	girl	4	PMID:23691375

Continued on next page

Table S2 – *Continued from previous page*

Disease	**Gene**	**Proband**	**n. HPO terms**	**Publication**
Holoprosencephaly 4	TGIF1	male proband	7	PMID:16962354
Candidiasis, Familial, 2	CARD9	Patient	8	PMID:26044242
Megaloblastic Anemia 1	AMN	III:1	3	PMID:26040326
Desmosterolosis	DHCR24	proband	34	PMID:29175559
Spastic Paraplegia 76, Autosomal Recessive	CAPN1	Family C-IV:13	3	PMID:27153400
Hypotonia, Infantile, With Psychomotor Retardation And Characteristic Facies 3	TBCK	1-2	8	PMID:27040691
Larsen syndrome	FLNB	19	12	PMID:16801345
Toe Syndactyly, Telecanthus, And Anogenital And Renal Malformations	CCNQ	Case 2	14	PMID:18297069
Loeys-Dietz syndrome 2	TGFBR2	Patient 4	15	PMID:30101859
Poikiloderma With Neutropenia	USB1	patient	7	PMID:27247962
Neuropathy, Hereditary, With Liability To Pressure Palsies	PMP22	Proband	7	PMID:29078790
Pierpont syndrome	TBL1XR1	seven year old male	29	PMID:28687524
Hemophagocytic Lymphohistiocytosis, Familial, 2	PRF1	8-year-old boy	6	PMID:28468610
Jervell And Lange-Nielsen syndrome 1	KCNQ1	family III-IV-5	4	PMID:29037160
Niemann-Pick Disease, Type C1	NPC1	The proband	14	PMID:27900365
Spherocytosis, Type 5	EPB42	proposita	5	PMID:7803799
Cutis Laxa, Autosomal Recessive, Type Iic	ATP6V1E1	PI:1	13	PMID:28065471
Multiple Endocrine Neoplasia, Type Iia	RET	DM patient	3	PMID:24331334
Polymicrogyria, Symmetric Or Asymmetric	TUBB2B	proband	18	PMID:28966590
Ataxia-Pancytopenia syndrome	SAMD9L	IV-1	5	PMID:27259050
Metabolic Encephalomyopathic Crises, Recurrent, With Rhabdomyolysis, Cardiac Arrhythmias, And Neurodegeneration	TANGO2	Subject 2	33	PMID:26805781
Myasthenic syndrome, Congenital, 22	PREPL	proband	18	PMID:29483676
Gaucher Disease, Perinatal Lethal	GBA	boy weighing 1690 g	7	PMID:15967693
Kabuki syndrome 2	KMT2D	3 month old boy	21	PMID:30509212
Charge syndrome	CHD7	B III-3	14	PMID:17661815
Mental Retardation, Autosomal Recessive 18	MED23	IV.8	7	PMID:30847200
Citrullinemia, Classic	ASS1	5	8	PMID:23099195
Long Qt syndrome 14	CALM1	Case 2	4	PMID:27374306
Nance-Horan syndrome	NHS	III:1	9	PMID:30642278
Palmoplantar Keratoderma, Punctate Type Ia	AAGAB	family 1:proband	4	PMID:28239884
Mental Retardation, Autosomal Dominant 21	CTCF	proband	28	PMID:28619046
Ventricular Tachycardia, Catecholaminergic Polymorphic, 3	TECRL	Patient 1	8	PMID:27861123
Immunoskeletal Dysplasia With Neurodevelopmental Abnormalities	EXTL3	C:II-1	12	PMID:28132690
Parkinson Disease 7, Autosomal Recessive Early-Onset	PARK7	proband	13	PMID:27460976
Cockayne syndrome A	ERCC8	Patient C	5	PMID:30200888

Continued on next page

Table S2 – *Continued from previous page*

Disease	**Gene**	**Proband**	**n. HPO terms**	**Publication**
Hypotonia, Infantile, With Psychomotor Retardation And Characteristic Facies 3	TBCK	II-3	21	PMID:27275012
Myopathy, Myofibrillar, 3	MYOT	patient	5	PMID:19458539
Codas syndrome	LONP1	Patient 1	8	PMID:25808063
Rett syndrome, Congenital Variant	FOXG1	Patient 3	9	PMID:28851325
Retinitis Pigmentosa With Or Without Skeletal Anomalies	CWC27	1:II-3	12	PMID:28285769
Cockayne syndrome B	ERCC6	Patient B	5	PMID:30200888
Mucolipidosis Iv	MCOLN1	6 year old boy	8	PMID:28620732
Chediak-Higashi syndrome	LYST	patient	14	PMID:28183707
Marfan syndrome	FBN1	Patient 3	4	PMID:30101859
Congenital Disorder Of Glycosylation, Type Iih	COG8	proband	27	PMID:30690882
Pseudoachondroplasia	COMP	II-1	9	PMID:27330822
Polymicrogyria, Bilateral Frontoparietal	ADGRG1	Family A, II:2	4	PMID:29707406
Dyggve-Melchior-Clausen Disease	DYM	Patient 2	7	PMID:24300288
Arthrogryposis, Distal, Type 9	FBN2	IV:7	6	PMID:30147916
Neurodevelopmental Disorder With Or Without Anomalies Of The Brain, Eye, Or Heart	RERE	Subject 9	21	PMID:29330883
Smith-Magenis syndrome	RAI1	SMS335	15	PMID:20932317
Inclusion Body Myopathy With Early-Onset Paget Disease With Or Withoutfrontotemporal Dementia 1	VCP	II-3	11	PMID:19208399
Neurodevelopmental Disorder With Or Without Anomalies Of The Brain, Eye, Or Heart	RERE	Subject 4	87	PMID:27087320
Bleeding Disorder, Platelet-Type, 15	ACTN1	proband	5	PMID:24069336
Encephalopathy, Neonatal Severe, With Lactic Acidosis And Brain Abnormalities	LIPT2	P1	16	PMID:28757203
Cleidocranial Dysplasia	RUNX2	III:3	10	PMID:24966961
Congenital Disorder Of Glycosylation, Type Iic	SLC35C1	Proband 1	20	PMID:24403049
Rubinstein-Taybi syndrome 2	EP300	38	26	PMID:29506490
Craniofrontonasal syndrome	EFNB1	3269	17	PMID:23335590
Brugada syndrome 1	SCN5A	proband	3	PMID:31590245
Amyotrophic Lateral Sclerosis 1	SOD1	patient	7	PMID:30236613
Spastic Paraplegia 76, Autosomal Recessive	CAPN1	R-III:1	5	PMID:27320912
Hypotonia, Infantile, With Psychomotor Retardation And Characteristic Facies 3	TBCK	D-II-1	27	PMID:27040692
Ehlers-Danlos syndrome, Classic Type, 2	COL5A2	patient	8	PMID:27656288
Birt-Hogg-Dube syndrome	FLCN	253	2	PMID:96481
Diarrhea 3, Secretory Sodium, Congenital, With Or Without Other Congenitalanomalies	SPINT2	two-month-old male	13	PMID:29575628
Robinow syndrome, Autosomal Recessive	ROR2	Patient 2	19	PMID:24932600

`original`	unaltered data from case report
`noise2`	two "random" HPO terms added
`noise2`*	like noise2 but the original terms were replaced by a randomly chosen parent term
`noise2`**	like noise2 but the original terms were replaced by a randomly chosen grandparent term
`allele`$^{-2}$	remove all pathogenic alleles (i.e., remove one allele for dominant and two for recessive). Otherwise do not change the data
`allele`$^{-2,**}$	remove all pathogenic alleles (i.e., remove one allele for dominant and two for recessive), replace all terms with a parent term and then add two noise terms
`terms-randomized`	replace all HPO terms by "random" terms
`biallelic`	limit the case reports to those describing autosomal recessive (biallelic) diseases
`biallelic`$^{-1}$	same as `biallelic` but one of two pathogenic alleles is removed
`not`	10 cases in which a negated ("not") finding is important to the differential diagnosis (Table S4)
`not*`	same as `not`, but all negated terms are removed

Table S3. Approaches to add noise to the case report data (Phenopackets).

Correct diagnosis	Differential diagnosis	Differentiating feature
Loeys-Dietz syndrome 4 [OMIM:614816]	Marfan syndrome [OMIM:154700]	Ectopia lentis [HP:0001083]
Tietz albinism-deafness syndrome [OMIM:103500]	Waardenburg syndrome, type 2A [OMIM:193510]	Heterochromia iridis [HP:0001100]
Hypochondroplasia [OMIM:146000]	Achondroplasia [OMIM:100800]	Trident hand [HP:0004060]
Osteogenesis imperfecta, type XII [OMIM:613849]	Osteogenesis imperfecta, type IV [OMIM:166220]	Dentinogenesis imperfecta [HP:0000703]
Spinal muscular atrophy with progressive myoclonic epilepsy [OMIM:159950]	Spinal and bulbar muscular atrophy of Kennedy [OMIM:313200]	Elevated serum creatine kinase [HP:0003236]
Myotonia congenita, dominant [OMIM:160800]	Myotonic dystrophy 1 [OMIM:160900]	Muscle weakness [HP:0001324]
Trichorhinophalangeal syndrome, type I [OMIM:190350]	Trichorhinophalangeal syndrome, type II [OMIM:150230]	Intellectual disability [HP:0001249]
GM1-gangliosidosis, type III [OMIM:230650]	GM1-gangliosidosis, type I [OMIM:230500]	Cherry red spot of the macula [HP:0010729]
Megalocornea 1, X-linked [OMIM:309300]	Glaucoma 3, primary congenital, A [OMIM:231300]	Abnormal intraocular pressure [HP:0012632]
Ectodermal dysplasia 9, hair/nail type [OMIM:614931]	Ectodermal dysplasia 1, hypohidrotic, X-linked [OMIM:305100]	Abnormality of the dentition [HP:0000164]

Table S4. Pairs of diseases whose differential diagnosis is defined in part by the absence of the phenotypic abnormality listed in the third column. For instance, Loeys-Dietz syndrome 4 is noted not to be characterized by ectopia lentis, while the phenotypically similar disease Marfan syndrome is [4]. In each case, the disease in the first column is explicitly annotated not to have the phenotype in question, and the disease in the second column is annotated to have the feature. These ten cases are included in the 384 case reports (Phenopackets) analyzed in this work.

Tool	First published	**VCF**	**HPO**	**Web**	**Shell**	**Assemblies**	**Last update**
eXtasy [5]	2013	✓	✓	✓	✓	hg19	2013
Exomiser [6, 7, 8]	2014	✓	✓	×	✓	hg19, hg38	2019
Phen-Gen [9]	2014	✓	✓	✓	✓	hg19	2014
PhenoVar [10]	2014	✓(a)	✓	✓	×	hg19	2017
BierApp [11]	2014	✓	✓	✗(no access)	×	hg19	2016
wANNOVAR [12]	2015	✓	✓	✓	×	hg19, hg38	2019
OVA [13]	2015	✓	✓	✓	×	hg19	2015
OMIM Explorer [14]	2016	✓	✓	✗(no access)	×	hg19	2016
QueryOR [15]	2017	✓	✓	✗(no access)	×	hg19	2016
GenIO [16]	2018	✓	✓	✓	×	hg19	2017
AMELIE/Phrank [17]	2019	✓	✓	✗(b)	×	hg19	2019
Phenoxome [18]	2019	✓	✓	✓	×	hg19	2019
DeepPVP [19]	2019	✓	✓	×	✗(c)	hg19	2019
MutationDistiller [20]	2019	✓	✓	✓	×	hg19	2019
PhenoPro [21]	2019	✓	✓	✗(no access)	×	hg19	2019

Table S5. Other tools for phenotype-driven exome/genome analysis. Symbols: ✓ The tool has the capability denoted in the column. × The tool does not have the capability denoted in the column. ✗ The publication describes the capability in question but it was not functional during the period of time this manuscript was being prepared (Sep.-Dec., 2019). Additional comments: (a) Requires registration, which is not working; (b) Web version of AMELIE not accepting jobs (attempted various times, October–December, 2020); (c) Install instructions failed on dependencies or docker file; (no access): Web server could not be accessed on multiple occasions.

References

[1] Sebastian Köhler, Marcel H Schulz, Peter Krawitz, Sebastian Bauer, Sandra Dölken, Claus E Ott, Christine Mundlos, Denise Horn, Stefan Mundlos, and Peter N Robinson. Clinical diagnostics in human genetics with semantic similarity searches in ontologies. *The American Journal of Human Genetics*, 85(4):457–464, 2009.

[2] Roberta Roncarati, Chiara Viviani Anselmi, Peter Krawitz, Giovanna Lattanzi, Yskert von Kodolitsch, Andreas Perrot, Elisa di Pasquale, Laura Papa, Paola Portararo, Marta Columbaro, Alberto Forni, Giuseppe Faggian, Gianluigi Condorelli, and Peter N Robinson. Doubly heterozygous LMNA and TTN mutations revealed by exome sequencing in a severe form of dilated cardiomyopathy. *European journal of human genetics : EJHG*, 21:1105–1111, October 2013.

[3] Satoko Kumada, Masaharu Hayashi, Kunimasa Arima, Hiroshi Nakayama, Kenji Sugai, Masayuki Sasaki, Kiyoko Kurata, and Michio Nagata. Renal disease in Arima syndrome is nephronophthisis as in other Joubert-related Cerebello-oculo-renal syndromes. *American journal of medical genetics. Part A*, 131:71–76, November 2004.

[4] Yskert von Kodolitsch and Peter N Robinson. Marfan syndrome: an update of genetics, medical and surgical management. *Heart (British Cardiac Society)*, 93:755–760, June 2007.

[5] Alejandro Sifrim, Dusan Popovic, Leon-Charles Tranchevent, Amin Ardeshirdavani, Ryo Sakai, Peter Konings, Joris R Vermeesch, Jan Aerts, Bart De Moor, and Yves Moreau. eXtasy: variant prioritization by genomic data fusion. *Nature methods*, 10:1083–1084, November 2013.

[6] Peter N Robinson, Sebastian Köhler, Anika Oellrich, Sanger Mouse Genetics Project, Kai Wang, Christopher J Mungall, Suzanna E Lewis, Nicole Washington, Sebastian Bauer, Dominik Seelow, Peter Krawitz, Christian Gilissen, Melissa Haendel, and Damian Smedley. Improved exome prioritization of disease genes through cross-species phenotype comparison. *Genome research*, 24:340–348, February 2014.

[7] Damian Smedley, Julius OB Jacobsen, Marten Jäger, Sebastian Köhler, Manuel Holtgrewe, Max Schubach, Enrico Siragusa, Tomasz Zemojtel, Orion J Buske, Nicole L Washington, et al. Next-generation diagnostics and disease-gene discovery with the Exomiser. *Nature Protocols*, 10(12):2004, 2015.

[8] Damian Smedley, Max Schubach, Julius O B Jacobsen, Sebastian Köhler, Tomasz Zemojtel, Malte Spielmann, Marten Jäger, Harry Hochheiser, Nicole L Washington, Julie A McMurry, Melissa A Haendel, Christopher J Mungall, Suzanna E Lewis, Tudor Groza, Giorgio Valentini, and Peter N Robinson. A whole-genome analysis framework for effective identification of pathogenic regulatory variants in Mendelian disease. *American journal of human genetics*, 99:595–606, September 2016.

[9] Asif Javed, Saloni Agrawal, and Pauline C Ng. Phen-Gen: combining phenotype and genotype to analyze rare disorders. *Nature methods*, 11:935–937, September 2014.

[10] Yannis J Trakadis, Caroline Buote, Jean-François Therriault, Pierre-Étienne Jacques, Hugo Larochelle, and Sébastien Lévesque. PhenoVar: a phenotype-driven approach in clinical genomics for the diagnosis of polymalformative syndromes. *BMC medical genomics*, 7:22, May 2014.

[11] Alejandro Alemán, Francisco Garcia-Garcia, Francisco Salavert, Ignacio Medina, and Joaquín Dopazo. A web-based interactive framework to assist in the prioritization of disease candidate genes in whole-exome sequencing studies. *Nucleic acids research*, 42:W88–W93, July 2014.

[12] Hui Yang and Kai Wang. Genomic variant annotation and prioritization with ANNOVAR and wANNOVAR. *Nature protocols*, 10:1556–1566, October 2015.

[13] Agne Antanaviciute, Christopher M Watson, Sally M Harrison, Carolina Lascelles, Laura Crinnion, Alexander F Markham, David T Bonthron, and Ian M Carr. OVA: integrating molecular and physical phenotype data from multiple biomedical domain ontologies with variant filtering for enhanced variant prioritization. *Bioinformatics (Oxford, England)*, 31:3822–3829, December 2015.

[14] Regis A James, Ian M Campbell, Edward S Chen, Philip M Boone, Mitchell A Rao, Matthew N Bainbridge, James R Lupski, Yaping Yang, Christine M Eng, Jennifer E Posey, and Chad A Shaw. A visual and curatorial approach to clinical variant prioritization and disease gene discovery in genome-wide diagnostics. *Genome medicine*, 8:13, February 2016.

[15] Loris Bertoldi, Claudio Forcato, Nicola Vitulo, Giovanni Birolo, Fabio De Pascale, Erika Feltrin, Riccardo Schiavon, Franca Anglani, Susanna Negrisolo, Alessandra Zanetti, Francesca D'Avanzo, Rosella Tomanin, Georgine Faulkner, Alessandro Vezzi, and Giorgio Valle. QueryOR: a comprehensive web platform for genetic variant analysis and prioritization. *BMC bioinformatics*, 18:225, April 2017.

[16] Daniel Koile, Marta Cordoba, Maximiliano de Sousa Serro, Marcelo Andres Kauffman, and Patricio Yankilevich. GenIO: a phenotype-genotype analysis web server for clinical genomics of rare diseases. *BMC bioinformatics*, 19:25, January 2018.

[17] Karthik A Jagadeesh, Johannes Birgmeier, Harendra Guturu, Cole A Deisseroth, Aaron M Wenger, Jonathan A Bernstein, and Gill Bejerano. Phrank measures phenotype sets similarity to greatly improve Mendelian diagnostic disease prioritization. *Genetics in medicine : official journal of the American College of Medical Genetics*, 21:464–470, February 2019.

[18] Chao Wu, Batsal Devkota, Perry Evans, Xiaonan Zhao, Samuel W Baker, Rojeen Niazi, Kajia Cao, Michael A Gonzalez, Pushkala Jayaraman, Laura K Conlin, Bryan L Krock, Matthew A Deardorff, Nancy B Spinner, Ian D Krantz, Avni B Santani, Ahmad N Abou Tayoun, and Mahdi Sarmady. Rapid and accurate interpretation of clinical exomes using Phenoxome: a computational phenotype-driven approach. *European journal of human genetics : EJHG*, 27:612–620, April 2019.

[19] Imane Boudellioua, Maxat Kulmanov, Paul N Schofield, Georgios V Gkoutos, and Robert Hoehndorf. DeepPVP: phenotype-based prioritization of causative variants using deep learning. *BMC bioinformatics*, 20:65, February 2019.

[20] Daniela Hombach, Markus Schuelke, Ellen Knierim, Nadja Ehmke, Jana Marie Schwarz, Björn Fischer-Zirnsak, and Dominik Seelow. MutationDistiller: user-driven identification of pathogenic DNA variants. *Nucleic acids research*, 47:W114–W120, July 2019.

[21] Zixiu Li, Feng Zhang, Yukai Wang, Yue Qiu, Yang Wu, Yulan Lu, Lin Yang, William J Qu, Huijun Wang, Wenhao Zhou, and Weidong Tian. PhenoPro: a novel toolkit for assisting in the diagnosis of Mendelian disease. *Bioinformatics (Oxford, England)*, 35:3559–3566, October 2019.